Author/s:
Xu, Yangmengfei

Title:
Inducing human movement pattern change

Date:
2021

Persistent Link:
https://hdl.handle.net/11343/311948

Inducing human movement pattern change

by

Yangmengfei Xu

ORCID: 0000-0003-4320-0064

Master of Philosophy

July 2022

in the

Department of Mechanical Engineering

Faculty of Engineering and Information Technology

THE UNIVERSITY OF MELBOURNE

A thesis submitted in total fulfillment for the

degree of Master of Philosophy

Abstract

Human's movement pattern shaping is widely used in neurorehabilitation and sports training. Recent studies have shown that robotic device has its potential to become an efficient tool for clinicians to induce this change. To understand human's movement, different computational models were proposed and studied to explain how human resolves their redundancy. Although some arguments are still existing, the general idea of optimization has been well accepted. Based on these computational models, the motor learning studies showed that through practice in the new environment, the reward-based optimization could drive human to search for a better movement pattern 1) to maximize the performance and 2) to minimize the motor cost. Leveraging this optimization idea in human motor learning, this work aims to induce the movement pattern changes in an experimental setup solely relying on the motor cost without any explicit kinematic error. In this strategy, the intervention space and adaptation space are decoupled: while the force field only applies to the hand linear velocity, the adaptation is expected to happen in the redundant arm joint space (*i.e.* the swivel angle).

This work, therefore, explores the following topics:

- Investigating the feasibility of inducing human motor adaptation in the redundant space by providing a task space intervention without explicit error feedback or instruction;
- Evaluating the contribution of a progressively changing goal in this implicit motor adaptation, assuming that this adaptation may be further promoted through subtle prompts to explore the cost space;
- Demonstrating a motor cost analysis based on the upper limb kinematics and dynamics model to validate the relationship between observations and motor cost.

Declaration of Authorship

I, YANGMENGFEI XU, declare that this thesis titled, "Inducing Human Movement Pattern Change Without Explicit Error Feedback: A Motor Cost Approach" and the work presented in it are my own. I confirm that:

- The thesis comprises only my original work towards the degree of Master of Philosophy except where indicated in the preface;
- due acknowledgement has been made in the text to all other material used; and
- the thesis is fewer than the maximum word limit in length, exclusive of tables, maps, bibliographies and appendices as approved by the Research Higher Degrees Committee.

Signed:

Date:

Preface

The work contained within this thesis has been completed with the support of the Australian Research Council Linkage Project LP180101074.

The work presented in Chapter 3 and 4 has been published by **IEEE Transactions on Neural Systems and Rehabilitation Engineering** on 12 July 2021.

Acknowledgements

In the past two years, I have received a great deal of support and assistance from many people.

First and foremost, I would like to express my sincere thanks to my supervisors Prof. Denny Oetomo, Prof. Ying Tan, Dr Vincent Crocher, and my "shadow supervisor" Dr Justin Fong for your countless hours of guidance and support from formulating the research problem to the completing this thesis. The discussions in our meetings pushed me to sharpen my thinking and polish my work. I'm very lucky to have such an approachable group of supervisors in the past two years.

Secondly, I would like to acknowledge my colleagues in the Human Robotics Lab — Ali, Jing, Ricardo, Raphael, Xiruo, Lawrence, Zeyu, Yu Xia, Xinliang and everyone in the lab. We had a great coffee time before the pandemic, and I've enjoyed those discussions on research, travelling, sports and many. Wish we'll have more in future.

I would also like to thank my committee chair Prof. Saman Halgamuge for your insightful feedback which helped me a lot in presentation and writing. Thanks also to Dr Marlena Klaic for kindly sharing knowledge in neurorehabilitation practice.

In addition, I would like to thank all the volunteers involved in the experiments for your kindly cooperation and time input.

Finally, I would express my deepest love to my parents. Thanks for giving birth to me in the first place and supporting my decision (like you always did) on returning to the campus and having this new journey. I count myself fortunate for that. I would also thank Jingwen. You gave me the courage and motivated me to climb this mountain. Also, thanks to Jialin for your help and support during this worldwide pandemic. In the end, I would like to express my grateful thanks to all my friends here and overseas for your time, help and smile.

Contents

List of Figures

List of Tables

Abbreviations

CG	**C**onstant **G**oal
CNS	**C**entral **N**ervous **S**ystem
DoF	**D**egree of **F**reedom
E	**E**lbow
ISC	**I**ndirect **S**haping **C**ontrol
KSC	**K**inematic **S**ynergy **C**ontrol
PG	**P**rogressive **G**oal
RoM	**R**ange of **M**otion
S	**S**houlder
TIFT	**T**ime-**I**ndependent **F**unctional **T**raining
TTI	**T**orque-**T**ime-**I**ntegral
UI	**U**ser **I**nterface
W	**W**rist

Constants

gravitational acceleration $g = 9.8\text{ms}^{-2}$

Symbols

d	distance	m
$\mathbf{f}$	force	N
l	length	m
m	mass	kg
q	joint angle	$^\circ$
$\dot{\mathbf{x}}$	hand velocity	$m \cdot s^{-1}$
θ	swivel angle	$^\circ$

Chapter 1

Introduction

The movement of the human body usually involves a high dimensional configuration on a set of coordinates, and it requires a high amount of information processing capacity [9, 10]. To achieve the movement goal without concentrating on the coordinates of each joint, human is keen to pack the configuration as a stable and reproducible pattern, namely movement pattern. Movement pattern shaping or modification is a relearning process to help humans change their learned pattern to the desired one (*i.e.* reaching a target with more or less elbow rotation). It is widely used in neurorehabilitation, physical therapy and sports training.

According to the World Health Organization, 15 million people suffer from stroke worldwide each year, and stroke is ranked as the second leading cause of death worldwide [11, 12]. Based on the data from the Australian Bureau of Statistics 2018 Survey of Disability, Ageing and Carers, more than 100 stroke events were reported in Australia every day in 2017 [13, 14]. One of the most critical areas affected by stroke is motor skills, usually presenting as unnatural movement patterns or pathological synergies. A typical example of these unnatural movement patterns is the unnatural shoulder elbow synergy. A stroke survivor who suffered from limited upper limb motor function needs to use the trunk to compensate the limb movement in a reaching task, which not only limits their abilities in daily life (*i.e.* limited Range of Motion (RoM)) but be harmful to those over-used

muscles in long-term compensations as well [15]. To improve their abilities and avoid secondary complications, movement pattern shaping is critical in the neurorehabilitation process. Besides, in physical therapy, movement pattern shaping which is an alternative option for surgical treatment also plays a critical role in reducing or avoiding a variety of musculoskeletal pain conditions [16–18]. For example, acetabular dysplasia is an orthopedic disorder that, in severe cases, can lead to fractures of the acetabular rim. The current standard treatment approach in adults is a Bernese periacetabular osteotomy (PAO), which aims to delay or prevent the onset of hip osteoarthritis (OA) by improving the coverage of the femoral head to reduce contact stress. However, a complication rate of 15% can be expected. Given the invasive nature of the surgery, movement pattern shaping which is an effective non-surgical treatment option for active adults with mild dysplasia is important [17]. Moreover, in sports training, movement pattern shaping could also help the athlete to avoid pain and improve their performance [19].

In tradition, movement pattern shaping usually relies on systematic verbal instruction, feedback and tactile intervention from the coaches or physiologists. Recently some research has focused on systematically study how to influence subjects to learn a different movement pattern using the physical intervention [4, 5]. In this case, the robotic device has the potential to become an efficient tool because of its advantages in accurate measurement and programmable physical intervention.

In the past few decades, robotic devices have been well developed and deployed in many fields, including medical and sports training applications. The robotic devices are able to provide consistent physical intervention output as well as accurate measurement compared to humans. Given that the robotic devices are programmable, the trainers are expected to customize the usage to optimize the therapy or training outcome based on trainees' situations. Thus, robotic device could potentially become an important tool for physiologists and coaches.

The typical robotic devices used in training or neurorehabilitation are exoskeletons and manipulandum robots [1]. The exoskeleton usually has matched linkage length and whose joint position aligns with body size. The intervention of exoskeleton is

applied to joint space directly to shape the joint kinematics. Specific to the upper limb reaching task, the direct intervention is usually applied on corresponding joints or limbs directly to shape or assist the arm movement. The manipulandum based robot usually only has one contact point between the robot and human, and the intervention is usually applied at contact point to shape the arm movement indirectly. The indirect intervention has its advantages in the simplicity of the device mechanical structure and setup, as the exoskeleton requires matched joint position and aligned linkage length with body size, while the manipulandum is suitable for different persons and does not require setup change. Specific to the movement pattern shaping study, it is hard to decouple the robotic contribution from the movement pattern generated by a human using a direct method with an exoskeleton, and the observation usually comes with a combination of the output from both robot and the subject. Moreover, the indirect method with a manipulandum based robot has better extensibility, as the redundancy of the human body is seen at different levels, and the movement pattern shaping could happen not only in joint kinematics but also muscle level, which is hard to be accessed directly via a robotic device.

The research focusing on movement pattern shaping using robotic devices has been studied not only with different types of robotic devices but also different types of instructions that can be mainly categorized into explicit instruction and implicit instruction. Explicit instruction means subjects understand the real objective is to shape the movements. In contrast, for the implicit instruction, the subjects are not aware of the true objective of the experiment. Suppose the study involved a healthy subject who is capable of changing their movement pattern consciously, it is essential to have implicit instructions to avoid the influence from subjectiveness (*i.e.* the participants trying to cooperate with the research objective) and isolate the outcome induced by the physical intervention only. In other words, either direct or indirect methods, relying on explicit instructions or description of the physical intervention (including an explicit kinematic error), cannot demonstrate the efficiency of such a physical interaction.

Most current studies on movement pattern shaping using physical interaction produced by robotic devices have either direct interventions [4, 5] or explicit instructions [4, 8]. It is worth investigating the feasibility of inducing the healthy subjects' upper extremity movement pattern change in a reaching task with an indirect intervention and implicit instructions, which could minimize the trainee's consciousness of the movement pattern change induced by the robotic device.

1.1 Problem Statement

The direct methods have the advantage of providing matching feedback at the corresponding joint and limb. With this approach, subjects can quickly adapt their movement pattern based on the feedback, even with implicit instructions. Unlike the direct method, in the indirect method, the intervention space should be completely decoupled from the adaptation space, and it thus works in the absence of any kinematic error feedback. The primary problem is thus proposed that "is it feasible to shape human's movement pattern in the redundant space by providing a task space intervention without explicit error feedback or instruction?". One of the most significant difficulties lies in the absence of both the kinematic error feedback and the consciousness, which requires an alternative method to induce the change. This thesis explores the feasibility of leveraging the motor control theory in literature to induce the desired movement pattern change in an indirect and implicit manner. In this work, we investigate this movement pattern change in an upper limb reaching task, as the human's upper limb which has more than sufficient degrees of freedom (DoF) to locate the hand position (known as redundancy). Such a movement pattern shaping strategy can be potentially used in rehabilitation of post-stroke patients, physical therapy, and sport training to improve the outcome.

Given that this movement pattern change can only rely on the change of physical intervention, some subtle prompts may be helpful, and thus a progressive goal could potentially promote the outcome in this case. A typical method is

to utilize a progressive goal in the task, and examples of such approach can be seen in neuro-rehabilitation, where recovery is not achieved suddenly but rather progressively [20, 21]. This progressivity could help to improve one's capabilities progressively when the limits of those capabilities are unknown. Therefore, the secondary problem is proposed: "Can the progressivity contribute to the outcome of movement pattern shaping in this indirect and implicit manner?"

1.2 Contributions and thesis structure

This thesis, therefore, aims to address the problems proposed in the previous section. Specifically, the three main contributions are

1. Investigating the feasibility of inducing motor adaptation in an upper limb point-to-point reaching task in the redundant space by providing a task space intervention without explicit error feedback or instruction, and empowering simple devices to be used in movement pattern modifications for highly redundant tasks [Chapter 3];

2. Evaluating the contribution of a progressively changing goal in this implicit motor adaptation [Chapter 4];

3. Demonstrating a motor cost analysis based on the upper limb kinematics and dynamics model to validate the relationship between observations and motor cost [Chapter 5].

The thesis is thus structured as following:

In Chapter 2, the existing motor control and motor learning studies are reviewed. Taking neuroplasticity as the theoretical basis, the rationale for introducing a progressive goal is presented. At last, the existing strategies and algorithms on movement pattern shaping with robotic devices are summarized, categorized, and reviewed in different dimensions. Generally, this chapter identifies the challenges

of an indirect and implicit shaping approach and proposes the hypothesis based on motor control and neuroplasticity theories. The subsequent chapters formalize how these challenges are to be addressed and how the hypothesis is tested.

Chapter 3 introduces detailed experimental methodology on leveraging the motor control theory to influence the movement pattern in an upper limb point-to-point reaching task without any explicit instruction or direct physical effect in the adaptation space. Then the corresponding results are presented, evaluated, and discussed. The outcomes of this chapter correspond to Contribution 1 and 2.

As the indirect method has an absence in the direct intervention and explicit instruction, it may be difficult for the subject to adapt their movement to the desired pattern. Thus, in Chapter 4, a new progressively changing goal is deployed into the shaping strategy introduced in the previous chapter. The detailed experimental methodology on how to involve this progressivity is described, followed by comparing the results between this new variation and the constant one. Then, the contribution of the progressivity is evaluated. The outcome of this chapter corresponds to Contribution 3.

As this indirect and implicit shaping strategy leverage the motor control theory and relies on an artificial change of the difficulty to finish a task at a certain pose, analysis of this cost based on an upper limb model is demonstrated in Chapter 5. This simulation analyzes the cost differences when performing a task in different poses when exposed to this new environment, and potentially explains the changes induced by the force field. This analysis aims to help interpret the observations from the experiment and validate the relationship between the observations and simulations.

Chapter 6 summarises the major observations in this study and proposes potential future research directions.

Chapter 2

Background

Human's movement involves a high dimensional configuration on a set of the co-ordinates of the relevant articulations in a given task [9] (examples can be seen in Figure 2.1). At a set of joint coordinates, different mechanical impedance can be performed by activating muscles at different intensities (*i.e.* co-contraction of a pair of muscles to increase stability, and examples can be seen in Figure 2.2) [22]. This high number of degrees of freedom (DoF) can also be found at other levels (*i.e.* task level and neural level). This high volume of information requires a high process capacity [10], but also brings high redundancy for human to perform a movement.

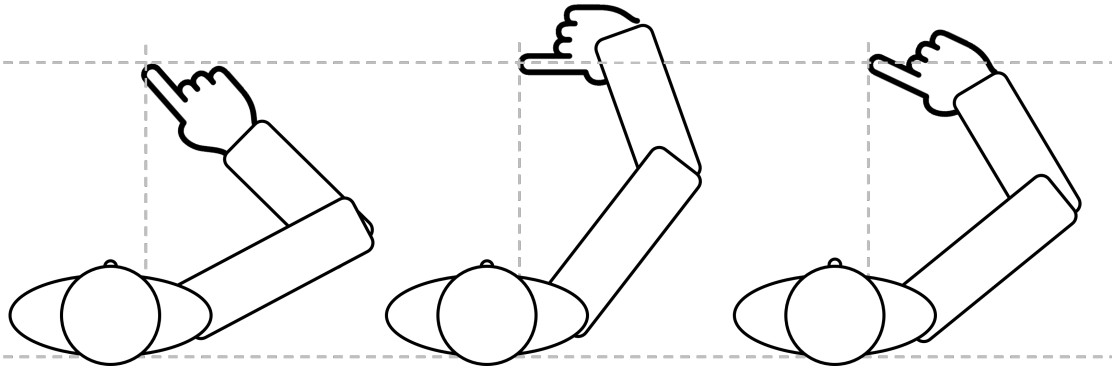

FIGURE 2.1: Examples of joint level redundancy in a simple 2D reaching task: for a given task space position, there are infinite possible joint configurations [1].

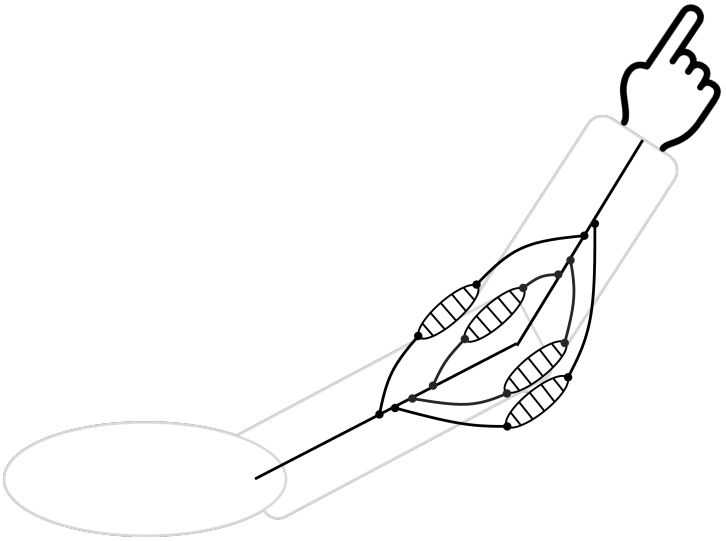

FIGURE 2.2: Examples of muscle level redundancy: for a given joint torque, there are infinite possible muscle force combinations (Note: diagram indicative only, does not represent actual muscle configurations) [1].

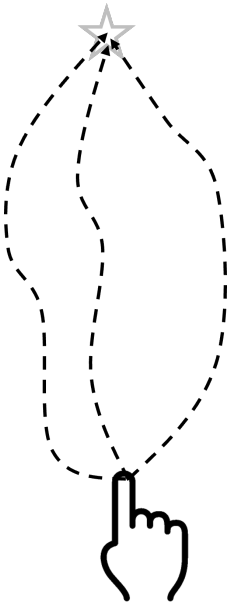

FIGURE 2.3: Examples of task level redundancy in a simple 2D reaching task: for a given task, there are infinite possible trajectories to reach the target [1].

In this chapter, three main topics are explored. First, an overview of human motor control is presented to explain how the redundancy is managed and selected. This is followed by a background in human motor learning to explore how this redundancy is influenced, and thus, new movement pattern learned. Finally, an introduction on the studies on influencing this redundancy using robotic devices is presented.

2.1 Human motor control

The human body provides us flexibility in performing the movement in different ways, but at the same time, brings a high volume of information to be processed in each movement. To reduce the amount of information needed to be processed during each movement, human packed these configurations into a stable and reproducible pattern — movement pattern (also known as synergy) — which allows us focusing on processing important information without concentrating on the coordinates of each joint and activation of each muscle during the movement. In general, movement patterns or synergies represent low-dimensional movement information expressed in a higher-dimensional space of possible activation [23].

The mechanisms of synergy formation at the neural level can be generally classified into two categories which are "anatomical synergies" and "functional synergies" [23]. The "anatomical synergies", as the name suggests, stands for multiple muscles that are activated at the same time based on their anatomical structures. The information from the motor cortex from the brain will be firstly sent to a module (*i.e.* a spinal module) and then be diverged to each muscle. Thus, the muscles would be activated at the same time. These synergies are usually considered to be "hard" as the anatomical structure has decided which muscles are involved in the synergy. In contrast, the "functional synergies" do not have their dedicated anatomical structures to physically connect to the muscles, providing human redundancies in completing a task in different ways. The formation of these synergies are purely based on functional coordination of high-dimensional

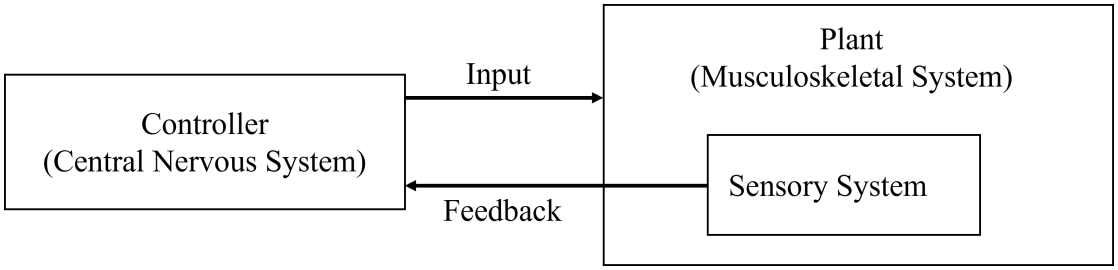

FIGURE 2.4: Controller and Dynamics representation of the human motor control system (Reproduce from [1]).

structures and are resulted from learning or training. The movement pattern is usually referred to this type of synergies which can be altered through training.

From engineering perspective, to produce a functional movement, the human must resolve this redundancy based on a mechanism or a computational model. To investigate this mechanism, a varies of studies have been performed in the past few decades to understand how human performs a well-mastered movement pattern. In these studies, the complex and nonlinear human musculoskeletal system, which includes bones, muscles, tendons, ligaments and soft tissues, is usually simplified to an input/output system from an engineering perspective, as shown in Figure 2.4. The actuation signal is sent from the Central Nervous System (CNS) (usually from the motor cortex from the brain and through the spinal module) to the musculoskeletal system to perform a movement, and then the feedback from senses, including visual and proprioceptive feedback, is sent back to the brain. After processing this feedback, the controller (CNS) will construct the new input and send it to the system. This process is a typical control loop from an engineering perspective.

However, modelling the human body is complex, and thus simplifications are always employed depending on the context and purpose of the models. Among them, the common opinion is that the human performs a movement as the results of some optimizations, but the form of the cost function and its elements are still arguable. Different models have been proposed and attempted to model this unknown cost function, and the common elements used are energy consumption and efforts [24–32]. They can be generally categorized into three main groups: Cost

function based on parameters of kinematics, mechanical dynamics, and neurological dynamics [1].

2.1.1 Cost function based on parameters of kinematics

A pilot study by Flash and Hogan on the motor cost in a reaching task in a horizontal plane introduced a cost function based on the jerk (the third derivative of position) of the hand movement [24]. The results showed that human tries to minimize the time integral of the square of jerk magnitude in reaching task either with constraint (*i.e.* obstacle avoidance during reaching) or without constraint. The optimum led to an approximately straight line when there is no obstacles between two points. In a later study on reaching tasks in three-dimensional space by Kim et al. [25], the human arm was modelled as a two-link seven degree-of-freedom (DoF) manipulator, and thus the swivel angle [33] (see Figure 2.5 and Figure 2.6 for details) is redundant to the positioning of the hand. As opposed to the task space optimization in Flash and Hogan [24], Kim et al's study shows that an optimization is required as the problem is redundant — not only in time and hand trajectory (minimum jerk) but also the joint configuration, when considering reaching but in joint space. These findings suggested that the optimization resolves the trajectory and configuration of the arm joints to make it easiest to move the hand towards the target.

However, this model cannot explain all scenarios in human's daily life. For example, putting a bottle with and without water onto a table following the same trajectory result in the same kinematics, but the muscle activation as well as the motor cost is different. In this case, the cost function based on dynamics parameters were developed at either mechanical level or neurological level.

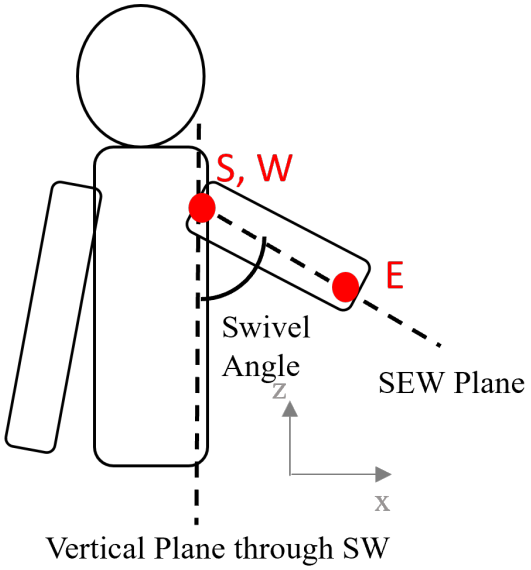

FIGURE 2.5: Front view of human body, where S, E, W represent joint of shoulder, elbow and wrist, and the swivel angle is the angle between the SEW plane and vertical plane through SW.

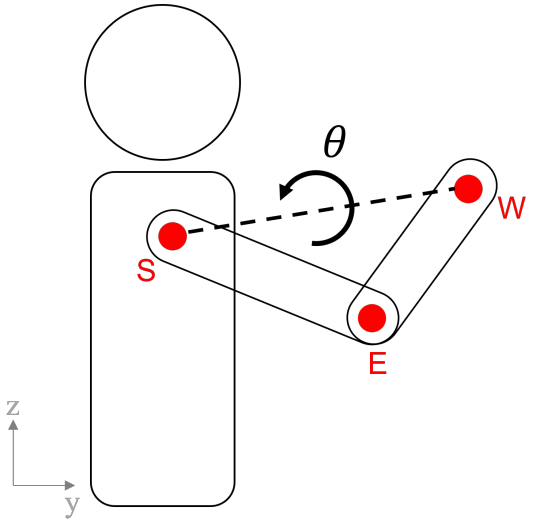

FIGURE 2.6: Side view of human body, where S, E, W represent joint of shoulder, elbow and wrist, and θ represents the swivel angle

2.1.2 Cost function based on parameters of mechanical dynamics

As mentioned at the beginning of this chapter, the redundancy of human movement is seen at different levels. The kinematics model could describe the movement completely, but it is not sufficient to define the motor control. Thus, the mechanical dynamics parameters are introduced into the cost function in recent studies to better explain human motor control. The studies on cost function based on mechanical dynamics optimizations usually involve parameters on work or torque at the joint level. In Kang et al.'s work [26], a two-link mechanism with a spherical joint for the shoulder and a revolute joint for the elbow is utilized, and the swivel angle (see Figure 2.5 and Figure 2.6) become the only redundant parameter in this model. For a given task space trajectory, the optimization in this model is to minimize the work done by the joints and resolve the only redundancy at the joint level. Similar to optimization on work, the optimization on torque change is also studied [27, 28]. The model used in these studies is a two-link manipulator with six muscles, and the redundancy is seen at both joint and task level. The formulation was first proposed in [27] and was revised in [28]. In the revised study, an updated minimum commanded torque change is also proposed, and it involves the viscous properties of the muscle, with which the commanded torque must overcome to move the limb. Comparing the cost functions fully relies on the kinematic parameters, the parameters of mechanical dynamics could better explain human behaviors with or without the same kinematics.

2.1.3 Cost function based on parameters of neurological dynamics

The previous cost functions explained the measurement and observations at kinematics and mechanical dynamic level, but in motor control, the input of the muscle is actually from the controller (CNS) and then sent to each muscle. In this case, the cost function based on neurological dynamics parameters that can represent

Reference	Parameters	Optimization class	Resolved redundancies
[24]	Jerk	Kinematic	Task
[25]	Swivel angle	Kinematic	Joint
[26]	Work of joints	Mechanical dynamics	Joint
[27] & [28]	Torque change	Mechanical dynamics	Joint, Task
[29]	Effort	Neurological dynamics	Joint, Task, Muscle
[30]	Motor signal	Neurological dynamics	Task, Endpoint
[34]	Motor signal	Neurological dynamics	Task, Time
[32]	Motor signal	Neurological dynamics	Time

TABLE 2.1: Summary of cost functions in human motor control literature (Reproduced from [1])

signals from the brain was studied in the past few years. In Guigon et al. [29], the muscle dynamics with a second-order low pass filter is modelled as a "neural control signal" or equivalent to "effort" which is penalized in the cost function. The optimization was used to describe the reaching tasks in 2D or 3D with or without wrist joints. This result agreed with the findings from Todorov and Jordan's [30] study and Harris and Wolpert's study [32] on the penalization on the motor command signal. Similar optimizations on neurological dynamics parameters can be found in [34], in which the time was not explicitly constraint.

In summary, different computational models have been proposed and attempted to explain how human resolves their redundancy with or without constraints. All of them agreed that the motor control is based on optimizing some cost functions, but the parameters in the cost function are still an open question. The mentioned literature is summarized in the Table 2.1.

2.2 Human motor learning

In this thesis, the motor control theory is defined on the studies which try to explain how human performs a well-mastered movement (*i.e.* a movement pattern or a synergy), while the motor learning studies try to explain how the human motor controller changes over time when in a new or changed environment. Motor learning plays an essential role in human's life. It helps us to master the skills

such as walking, writing, using tools. Moreover, the studies showed that it also plays an important role in neurorehabilitation to help persons with impaired motor function improve their abilities [35–38].

As the saying "Practice makes perfect", motor learning helps human to improve their abilities or performance in a given task. From the engineering perspective, motor learning is the process that the human motor controller approaches to an optimum of a cost function to maximize the performance or minimize the effort. It is noted that it is hard to isolate the motor learning from motor control study, as in many motor learning studies based on the computational models, the observations still ended with a repeatable pattern that is thought as an optimum referred to the optimization behaviour in motor control theory. In this section, motor learning will be discussed in two parts which are skill acquisition — learning a new task (*i.e.* utilise equipment, play new sports) and motor adaptation — adapting to an external or internal environment change in a known task (*i.e.* walking on ice, walking after swimming).

2.2.1 Skill acquisition

When human acquiring new skills, it usually requires human to practice many times until they master the skills well. From a computational model perspective, this process is the controller to find the optimum with respect to this new motor task and configure the patterns. In the studies on the computational model of skill acquisitions, motor learning is usually indicated or modelled based on the performance improvement over time, such as time reduction in completing the task, error reduction in each trial or success rate in completing a task [39–41]. One of the most classic experiments was conducted in the early last century, and the results showed that the performance improvement in a tracing task obeyed the math model of the power law [42]. These studies can mathematically describe the observations in the experiment and provide a prediction on learning behaviour in a specific task. A framework based on neurological aspects was proposed to

investigate the general learning behaviour that can apply in different tasks [43]. In this framework, motor learning was suggested to be driven by both reward and error. Similar results were observed in another experiment [44], in which the cost function was modelled as a weighted sum of kinematic error and effort.

2.2.2 Motor adaptation

The motor adaptation usually refers to the optimum change in motor cost function due to the internal or external environment change. For example, humans may feel "heavier" when they walk after long swimming. As the water can provide a "gravity compensated" environment, this environment will change after we are back on land, and thus we need a short period of time to get used to the environment.

In many motor adaptation studies, the participants are asked to perform a reaching task attaching to a handle-based planner manipulandum device which would change the mechanical dynamics by providing a force field. This force field can be a static, stochastic, or random disturbance in the movement. To resolve this unexpected change, human would adapt their movement iteratively until they reach a stable pattern to reject the disturbances [45]. A typical observation in these motor adaptation experiments is the after effect — the sudden removal of the force field will usually lead to an "overshoot" in trajectory. Besides the mechanical dynamics, with a specific setup, the apparatus could also disturb the visual feedback of the human (*i.e.* an intentional error in visual feedback [46]).

From the computational model perspective, based on the observations, the motor learning process is usually modelled to a control loop based on the states and inputs [47–49]. The "state" is usually related to the performance and the "input" or "feedback" are from the sensory system. The combination of "state" and "feedback" are usually unique to a specific task and cannot be generalized into different tasks. In this perspective, motor adaptation can be thought of as how motor control changes in response to disturbances external or internal to the body.

It is noted that the reference trajectory is not always defined in the motor adaptation experiment. If the reference trajectory is provided, the error between the movement and the reference trajectory will become an indicator of the performance [45, 50]. Otherwise, other performance indices (*i.e.* success rate, completing time) and the effort will take heavier weight in the cost function [51]. In Izawa's work, a zero-mean stochastic force field (changing from trial to trial) was introduced into the environment, and the results showed that human can take this uncertainty into account, and adapted their movement to a new optimum. This optimization was not to cancel all perturbations from the robotic device, but a process of re-optimization to minimize this "implicit motor costs" which is not related to the task success and instructions [52].

In summary, the motor learning literature studies that through practice in the new environment, the reward-based optimization could drive human to search for a better movement pattern 1) to maximise the performance and 2) to minimise the motor cost.

2.3 Explicit and implicit learning

In the human brain, two general processes are engaged — the explicit and implicit. The explicit process is strategic and effortful while the implicit process is more intuitive and automatic [53]. In human motor learning, both explicit and implicit processes take place. For example, after shooting a basketball that missed to the right of the basket, one could strategically aim to the left for the next shoot. But, it can also happen that if one continues to aim at the basket, the ball would be progressively close to the center of the basket. The study of explicit and implicit motor learning has seen a recent surge in interest.

The explicit process can be formed quickly and is directly accessible to consciousness [54], while implicit motor learning is the development of the motor skills

through practices incrementally over time and is not directly accessible to consciousness [55]. Implicit adaptation is thus thought of as a systematic change occurring without conscious awareness. A pilot study showed that in a complex fine-motor catching task, uninstructed subjects performed better than explicitly instructed subjects [56]. Similar results were observed in [57] and [58], suggesting that the explicit strategy significantly attenuated motor learning. Patton and Mussa-Ivaldi, in later research, also demonstrated that implicit motor learning, which reinforces the learning process with minimal instructions, no knowledge of, and little attention to the trajectory, could potentially lead to better retention compared to explicit motor learning [59]. These results suggested that implicit motor learning has the potential to be applied in training motor skills in sports and neurorehabilitation [59]. These results are confirmed by M. Smith et al. in a series of experiments [60–64]. Significant and prolonged after-effects of implicit motor learning were observed after the experimental environment had been removed. They suggested that these systematic changes in motor output brought from implicit motor learning could persist.

However, applying implicit adaptation in neurorehabilitation is still arguable. Boyd and Winstein showed that the capacity of implicit motor learning might be impaired in stroke patients. In their experiment, a serial reaction time task that requires subjects to push the button corresponding to light as fast as possible is used to test the learning progress. The results showed that stroke patients who had been explicitly informed of the light sequence performed better than patients without prior knowledge, suggesting that providing explicit information about the task could attenuate motor learning deficits [65].

To better understand the relationship between implicit and explicit processes, Mazzoni and Krakauer designed an experiment to set up a conflict between implicit and explicit processes by instructing subjects to counter a visuomotor rotation using a cognitive strategy in a pointing task [66]. The results suggested that explicit strategies cannot substitute for implicit adaptation and are overridden by the motor planning system. The newest study also demonstrated that the explicit

strategy and implicit adaptation could synergize in a dynamic environment, but implicit adaptation showed to cancel the explicit strategy in a stable or slow-changing environment [53].

In summary, human motor learning includes both explicit strategy and implicit adaptation, and implicit adaptation is thought to be a systematic change that can last longer. Although extending these results to training for stroke patients in neurorehabilitation is still arguable, the contribution of implicit motor learning for healthy subjects is confirmed and suggested.

2.4 Movement pattern shaping

In neurorehabilitation, movement pattern shaping plays a critical role to help the impaired person to re-learn the motor functions. Given the high demand in movement pattern shaping, especially for upper limb reaching tasks, in various applications, researchers tried to systematically study how to influence subjects to learn a different movement pattern using an accurate, repeatable and consistent physical intervention [4, 5]. A potential solution is to use the robotic devices that can provide accurate measurement as well as consistent and programmable force output. The common robots used in the human motor study can be classified into two types: the exoskeleton and robotic manipulandum [67].

2.4.1 Movement pattern shaping using exoskeletons

Exoskeletons usually have matched joint position and linkage length with the users, and their kinematics are aligned with the users' skeletal system. Examples of exoskeletons include the ARMin [3], the ArmeoPower (Hocoma, Switzerland) and the ABLE platform [2]. They were able to work in 3D space and can provide direct kinesthetic feedback at corresponding joints and limb segments.

FIGURE 2.7: Rendering of ABLE-7 axis [2].

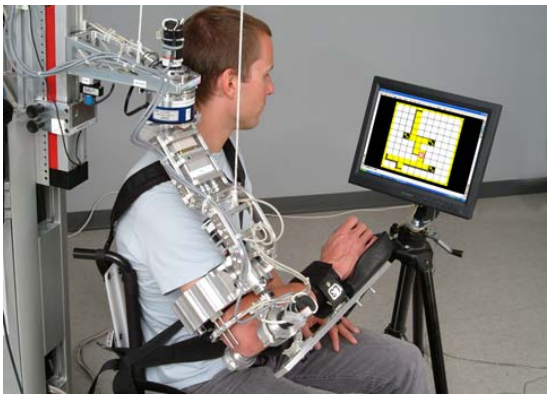

FIGURE 2.8: ARMin prototype [3].

FIGURE 2.9: ArmeoPower Exoskeletons (Hocoma, Switzerland).

As the exoskeleton is able to influence the specific joint or limb, shaping using an exoskeleton is well studied. In [4], a shaping strategy, named Time-Independent Functional Training (TIFT), was developed and deployed based on an exoskeleton device. The idea is to pre-define a desired shoulder-elbow synergy and a boundary wall to prevent the subject from moving outside this desired trajectory. The results showed that after eight training blocks, the trainees are able to perform the synergy with less blocking, and significant learning was observed. It is noted that all subjects are healthy subjects who are capable of changing their movement pattern. And the trajectory boundary made the desired synergy become explicit to all subjects.

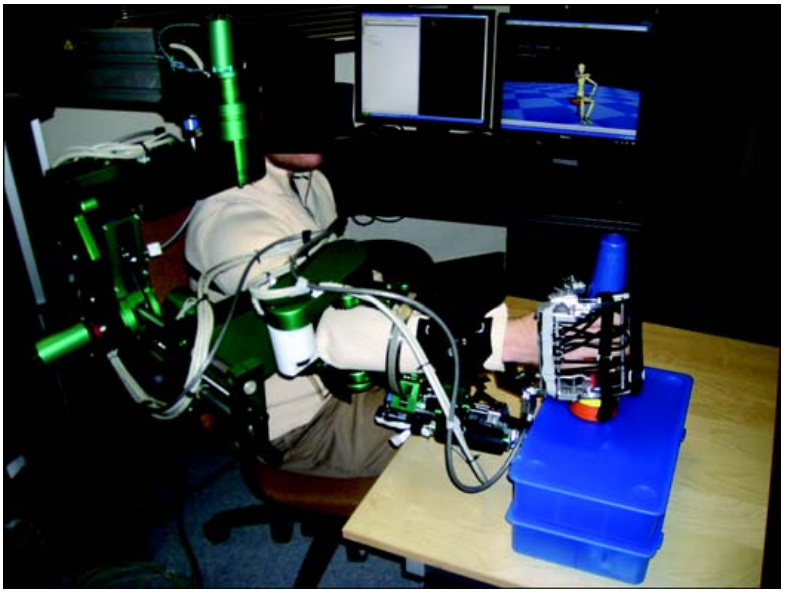

FIGURE 2.10: Experiment setup in [4] with ARMin III robot and passive hand device.

To avoid the influence from subjectiveness (*i.e.* the participants trying to cooperate with the researchers) and isolate the outcome induced by the physical intervention only, another study was performed by Proietti et al. [5]. In this study, the shaping strategy, namely Kinematic Synergy Control (KSC), was developed. KSC is a controller that could generate reactive viscous joint torques applied on multiple upper limb joints. Similar to TIFT, it has a pre-defined shoulder-elbow synergy, and the robot would apply the viscous torque to the corresponding joints based on the difference between measured movement and desired movement. There is no explicit instruction on movement pattern shaping in this study. Significant adaptation and after effect were observed in this study. The results suggested that an implicit adaptation of movement redundancy using a viscous force field was possible. Regrettably, there is no awareness check after the experiment to confirm this implicit manner during the experiment. Another difference between TIFT and KSC is the variety of tasks and generalization. TIFT constrained the hand trajectory and restrict the movement to one reaching target whereas there is no such restriction in Prioretti's work and they observed the generalisation of the learned coordination to untrained reaching tasks.

The exoskeleton has its advantages on high accessibility, but the drawback is also

FIGURE 2.11: Experiment setup in [5] with ABLE exoskeleton.

significant. It requires a perfect alignment for each subject to match kinematics. Otherwise, it may restrict the user's movement. This requirement brings a more complex setup than a manipulandum-based robotic device and thus limits its applications. From mechanical structure, given the exoskeleton usually has serial kinematics, high torques are needed at various joints. Thus, the mechanical inertia is at a high magnitude and distributed along the limb. This is usually called low dynamic transparency. To resolve problem, the motor used in the exoskeleton usually has a high gear ratio which reduces the backdrivability of the robot [67]. As a result, many of the motor adaptation studies involved 2D planner manipulandum devices to produce the force field.

2.4.2 Movement pattern shaping using robotic manipulandum

The robotic manipulandum requires only one attaching point (which is usually a handle) to provide the intervention. Examples of manipulandum include MIT Manus [68] and the MIME [7]. This simpler setup brings a high flexibility but also prohibits its access to the joints. Due to this nature, the robotic manipulandum is usually used to investigate the sensorimotor learning in end effect position control or shape human's task space trajectories [37, 69–73].

Thus, for movement pattern shaping at the joint level, limited studies were performed. A pilot study was seen in [8]. In their study, TIFT (see 2.4.1) was deployed on the Force Dimension Delta-6 manipulandum-based robot with 6 DoF, but only three positional axes were active during the experiment. Three healthy subjects were required to move with the desired pattern while attached to the

FIGURE 2.12: MIT-MANUS [6].

FIGURE 2.13: MIME workstation with PUMA-560 robotic arm in a therapeutic exercise [7].

robot device. Based on the joint position feedback from Kinect (a vision-based sensor to measure the joint angle), the robot would block the movement if the shoulder-elbow synergy was not desired. The results suggested that this method could encourage specific movement strategies. However, as mentioned in the previous section, the required pattern is made explicitly clear to subjects, limiting the conclusion drawn from the study. In another study, Valdes et al. [74] also used indirect force feedback with a similar objective. In their study, a force field at hand as a function of trunk compensations was shown to be able to reduce the trunk compensation in stroke survivors when doing a one-dimensional reaching task. This demonstrates the feasibility of shaping human's movement pattern indirectly, even if in that case, the force field was coupled to explicit instructions and feedback to the subjects.

Manipulandum device has a simpler mechanical structure and more straightforward setup compared with exoskeleton. Also, with the manipulandum-based robot setup, it is possible to fully decouple the intervention space (*i.e.* the hand task space) in which the intervention is applied from the motor adaptation space (*i.e.* the redundant arm joint space). With this method, the force to be exerted by the robotic system is not required to match the adaptation space, and so it has the advantages of simplicity and generality of application (*i.e.* a handle-based manipulandum device can be used to induce a motor adaptation expressed at the joint level, not physically controlled). In addition, because the adaptation space

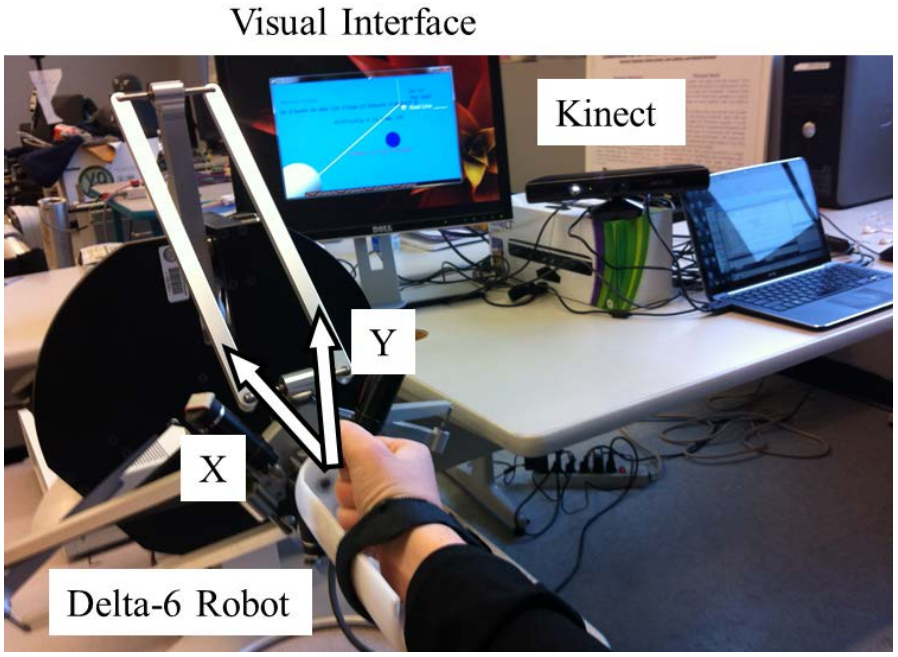

FIGURE 2.14: Experiment setup in [8] with DELTA-6 manipulandum robot.

is decoupled from the intervention space, the adaptation is purely driven by the subjects, and not a combination of the robotic and the subject inputs. Indeed, decoupling the adaptation space from the intervention space ensures that the subjects actually learn to produce the motor command required to achieve the task and not a complement to the force field. This indirect approach might thus be relevant in neuro-rehabilitation scenarios where re-learning of correct and efficient movement patterns plays an important role [75].

2.5 Summary

In summary, different computational models were proposed and studied to explain how human resolves their redundancy with or without constraints. Although some arguments are still existing, the general idea of optimization has been well accepted. Based on this process, human can adapt their movement to an optimized pattern with some cost function that is related to performance and effort. Looking at human motor learning from the engineering perspective, it studies that through

practice in the new environment, the reward-based optimization could drive human to search for a better movement pattern 1) to maximise the performance and 2) to minimise the motor cost. Leveraging this idea, in the movement pattern studies, the goal is usually to influence human's movement towards the desire through interventions from robotic devices. The studies on movement pattern shaping in a direct manner using exoskeleton devices have been studied in both explicit and implicit manner, and the outcomes are significant. However, studies on indirect shaping using manipulandum device at joint level is limited. It is worth investigating its feasibility, given its advantages.

As such, this thesis will explore the feasibility of inducing human movement pattern change indirectly and implicitly by leveraging the motor control theory. Thus, a task space intervention that aims to change human motor cost only will be provided to shape the joint space (redundant space) movement pattern without explicit error feedback or instruction. This indirect shaping strategy could empower simple devices (such as manipulandum) to be used in movement pattern modifications for highly redundant tasks. As suggested from the principle of neuroplasticity, progressivity will be deployed in the force field in the second experiment to explore the contribution of a progressively changing goal in this implicit motor adaptation. Finally, a computational model associated with the experiment data will be constructed to examine the motor cost change and explain the observations.

Chapter 3

Inducing human motor adaptation solely relying on motor cost

In Chapter 2, the advantages of shaping human's movement pattern in an indirect and implicit manner was introduced. To induce a desired movement pattern, a task-space force field which can encourage the motor adaptation in redundant space is to be designed leveraging the motor control theory. Recent works showed that human motor control involves the optimisation of a motor cost consisting of the combination of two components: one related to performance/error and one to energy/effort as highlighted in [44]. As summarized in Chapter 2, through practice in the new environment, the reward-based optimisation could drive human to search for a better movement pattern 1) to maximise the performance and 2) to minimise an "implicit motor cost" (here defined as the motor cost not related to the task success and/or instructions) [52].

This chapter explores the idea of driving indirect and implicit motor adaptation solely relying on the second component: the energy/effort. Specifically, the adaptation relies on the exploration of the cost space by the subject (through natural

variability in performing the task), which is expected to drive the indirect adaptation towards a new optimum instinctively. At the same time, the intervention is only applied at the task space without perturbing the adaptation in redundant space. This adaptation is hypothesised to occur without any explicit kinematic error feedback — instead, relying only on the subjects' attempts to minimise effort in performing the task, as perceived by their proprioceptive feedback. Thus, the approach introduced in this chapter is designed to be in an indirect and implicit manner: with the subjects having no intervention to contribute or prevent their movement in redundant space and with the subjects having neither instruction nor indication regarding the preferred movement.

This approach, named Indirect Shaping Control (ISC), has been previously experimented with five subjects by Fong et al. [76]. Results showed that healthy subjects adapted their movements unconsciously, however, the resulting changes to the subjects' movements were not always in the expected way. Two potential influences were noticed: a) physical contact point was at the center of the wrist; b) the original movement pattern was modelled in a linear relationship on constant mean value. The first factor may potentially prevent a fully free movement around the swivel angle for the subjects due to this physical constraint at the wrist. And the second factor may have led to a more artificial linear swivel angle change along the trajectory. As an extension of [76], in this project, the ISC strategy is modified to be applied at hand rather than wrist, and in the form to better respect to the natural movement pattern.

To test this hypothesis, a three-dimensional reaching task was selected. During the intervention phase, a force field, which opposed to the hand movement and only increased the movement effort, was applied at the hand. The amplitude of this viscous resistance was set as a function of the arm swivel angle (see Figure 3.2). The adaptation was thus expected to happen in the arm joint null space, parametrised by the swivel angle. Intervention effect was thus measured as the increase of the swivel angle during the intervention phase. Observations on a potential after effect were also performed using the same metric.

3.1 Experimental methodology

To validate the effectiveness of ISC, an experiment is thus designed. In this experiment, the hypothesis is that it is feasible to induce motor adaptation in the redundant arm joint null space by providing a task space intervention without explicit error feedback nor instruction using ISC approach. To test this hypothesis, a three-dimensional reaching task was selected. During the intervention phase, ISC is applied at hand. The amplitude of this viscous resistance was set as a function of the arm swivel angle as introduced in the previous section. The adaptation was thus expected to happen in the arm joint null space, parametrised by the swivel angle. Adaptation effect was measured as the increase of the swivel angle during and after the intervention phase.

$\theta_{goal}(i)$ is set to a constant value of 10° across all iterations in the intervention. A final goal of 10° increase was empirically selected after preliminary testing, to be both large enough to be observable as well as outside normal variability of movement and small enough to keep the change not noticeable by the subjects.

3.1.1 Participants

Five female and five male subjects (age: 23.7±4.0) participated in this experiment. All of these subjects were right-handed and did not suffer from any impairment in their upper-limb motor functions in past two years.

This experiment was approved by the University of Melbourne Human Research Ethics Committee (#1749444), and an informed written consent was received from all subjects.

3.1.2 Task design

In this experiment, the objective of the robotic intervention was to increase the swivel angle (see θ on Figure 3.2) with which the subject was performing reaching

tasks using his/her dominant hand.

Participants were required to sit on a fixed chair and repeat a reaching movement from their lap to a touch screen positioned in front of them as shown on Figure 3.1. The targets were shown on the centre of the screen and subject was asked to touch the target at his/her own pace. The location of the touch screen was normalised for each subject such that the height of the upper edge of the touch screen aligned with his/her chin and that his/her metacarpophalangeal joint was touching the screen when they fully extend his/her arm. Within this setup, when the subject touches the button on the screen, his/her arm was not fully extended.

During the experiment, in order to further encourage an implicit learning method, a quiz game was designed to distract the subjects from the exact objective of the study. The quiz User Interface (UI) was displayed on the touchscreen with the reaching target corresponding to the quiz answers. Answer buttons were assigned randomly and setup closely to one another (within a 5 cm radius) to minimise any target position effect. No time limitation nor timing instructions were imposed to participants who were performing the reaching task at their own comfortable pace.

The swivel angle was selected for its simple representation of the arm null-space on which the robotic device is incapable of direct physical effect (the EMU, displayed on Figure 3.1, being only able to apply 3D forces at the hand) and which configuration does not produce any kinematic error in reaching tasks. The swivel angle also accounts for a large part of the motor cost during reaching movements: the gravitational load applied to the arm (and so shoulder joints) increases while the elbow raises outside of a parasagittal plane.

3.1.3 Apparatus and measurements

In this experiment, the EMU, a three-dimensional end-effector based rehabilitation robotic device [67], was used to generate the ISC force field. The EMU

possess three active joints, with the ability to produce linear forces in the three directions, and is terminated with a passive ball joint unit, allowing free, unconstrained rotations. The subject's hand held the handle of the device, attached to the passive unit, with their wrist strapped, preventing wrist flexion/extension and abduction/adduction. This configuration allows the device to produce a force interaction in 3D whereas the orientation of the forearm is left free to rotate, thus producing no torque around the swivel angle axis (see [77] for a detailed kinematic analysis).

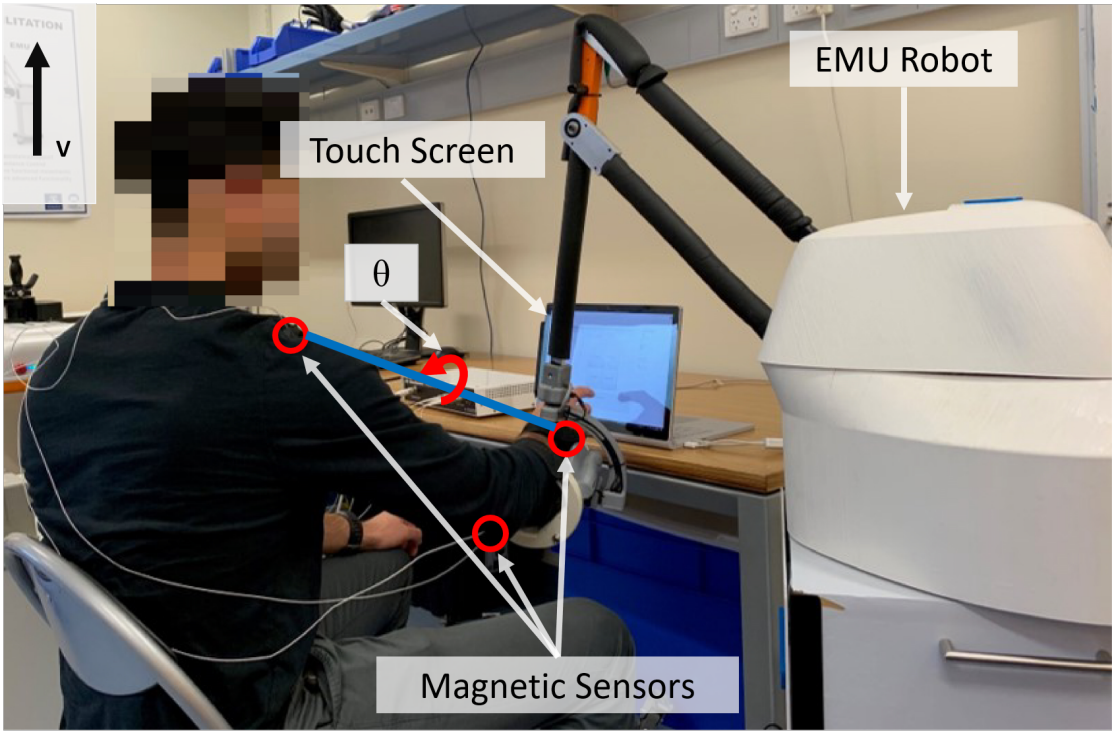

FIGURE 3.1: The experimental setup with the EMU manipulandum, the location of the three positions magnetic sensors and the swivel angle representation (θ), where $\mathbf{v}$ is an absolute vertical unit vector

TrakSTAR 3D Guidance Magnetic Sensors (Ascension Technology Corporation, USA) was used to measure the subjects' shoulder (S), wrist (W) and elbow (E) positions, which was subsequently used to calculate online the swivel angle as follows.

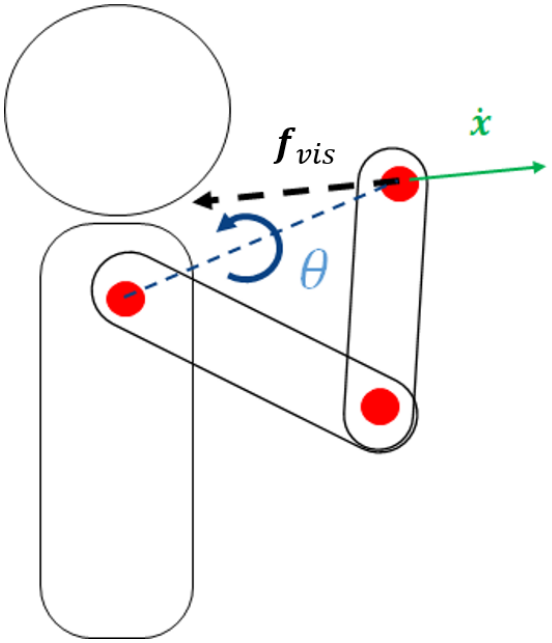

FIGURE 3.2: The schematic of the task with the swivel angle representation (θ), hand velocity ($\dot{\mathbf{x}}$) and corresponding viscous force field ($\mathbf{f_{vis}}(\theta, \dot{\mathbf{x}})$).

Vectors $\overrightarrow{SE}$ and $\overrightarrow{SW}$ were calculated using S, E and W positions and a normal vector to the SEW plane was expressed as:

$$\mathbf{n}_{arm} = \frac{\overrightarrow{SE} \times \overrightarrow{SW}}{\left\| \overrightarrow{SE} \times \overrightarrow{SW} \right\|_2} , \tag{3.1}$$

where $\|\circ\|_2$ denotes the L_2 norm.

Then, assuming the subjects maintained their trunk upright, the swivel angle can be calculated as [26]:

$$\theta = \arcsin\left(\mathbf{n}_{arm} \cdot \mathbf{v}\right) , \tag{3.2}$$

with $\mathbf{v}$ an absolute vertical unit vector.

The sensors position have an RMS error of 1.4mm. This results in an RMS swivel angle measurement error of 0.8° in the worst configuration.

The EMU's real-time controller (a sbRIO-9637, National Instruments Corporation, USA) was connected to a laptop which performed the force field computation

based on the swivel angle value and displayed the interface on a touch screen. All software was customised and written in LabVIEW (National Instruments Corporation, USA) at a 20Hz sampling rate.

Additionally, the swivel angle as well as the sensors positions and velocities (obtained through differentiation) were recorded during the experiment for post processing.

3.1.4 Revisit of Indirect Shaping Control (ISC)

Indirect Shaping Control (ISC) was previously introduced in [76]. In this pilot work, the movement pattern was characterised by the swivel angle, and a viscous field was applied to the subject's hand movement, as a function of the current swivel angle value. This viscous field was designed in such a way that the further the swivel angle θ is from the desired value $\theta_d(\cdot,\cdot)$, the more the force field increases the resistance. Such a setting artificially increases the movement cost (by increasing the viscosity), the further away the movement pattern is from a desired value.

In order to take into account inter-subject natural movement variability, the desired swivel angle $\theta_d(\cdot,\cdot)$ is designed based on each subjects' original swivel angle over the course of movement, identified during natural movements. For each user, this reference $\theta_o(d)$ was identified as a third-order polynomial of the distance to the reaching point (d) by fitting the data using a bisquare method.

For each iteration of the intervention i, an alteration goal of the swivel angle, denoted $\theta_{goal}(i)$ was defined.

In order to not influence the static posture of the subject at the initiation of movement ($d = d_0$), $\theta_{goal}(i)$ was linearly increased along the movement reaching path, starting with the subject's original posture and ending with the maximum change for the given iteration ($d = d_{max}$).

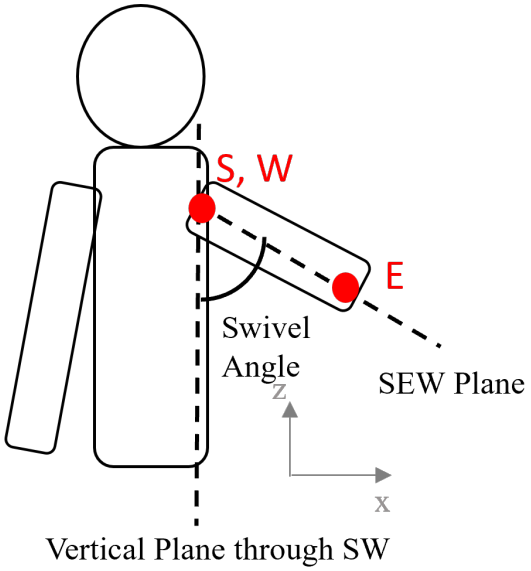

FIGURE 3.3: Front view of human body, where the swivel angle is the angle between the SEW plane and vertical plane through SW.

Namely, the personalised desired swivel angle $\theta_d(d, i)$ in iteration i and at a distance d from the starting point was defined as:

$$\theta_d(d, i) = \theta_o(d) + \frac{d}{d_{max}} \cdot \theta_{goal}(i) \ , \tag{3.3}$$

where d_{max} is the distance from the starting point to the target.

For simplicity of notation, $\theta_d(\cdot) = \theta_d(\cdot, i)$ or θ_d is used in this thesis when no confusion arises.

The force field thus relies on a swivel angle (the angle to represent the elbow rotation, see Figure 3.3 and Figure 3.4 for details) difference between θ_d and measurement θ. The force applied by the device at the subjects' hand is calculated as:

$$\mathbf{f}_{vis} = \begin{cases} -b_i \cdot b_k \cdot (\theta_d - \theta) \cdot \dot{\mathbf{x}} & , \text{ if } \theta_d > \theta \\ 0 & , \text{ otherwise} \end{cases} \tag{3.4}$$

where

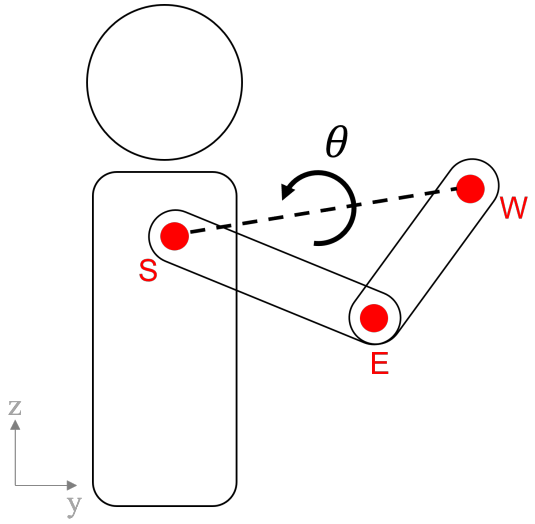

FIGURE 3.4: Side view of human body, where θ represents the swivel angle

- $\mathbf{f}_{vis}$ is the vector of the force applied at the end effector;
- $\dot{\mathbf{x}}$ is the vector of the real-time hand velocity in $m \cdot s^{-1}$;
- $\theta_d - \theta$ is the real-time difference between a desired swivel angle θ_d and the measured swivel angle θ (in degrees);
- b_i is a scalar factor changed according to the current iteration i and which aims to introduce and remove the viscous field gradually during the intervention. In all experiment in this thesis, b_i increases linearly from 0 to 1 in the first 15 iterations in the intervention and decreases linearly from 1 to 0 in the last 15 iterations in the intervention. b_i remains at 1 in the other iterations;
- b_k is a constant tuning gain to make the force field within a reasonable range and has been empirically set to $5000N \cdot s \cdot (m \cdot^{\circ})^{-1}$ in all experiments presenting in this thesis for all subjects.

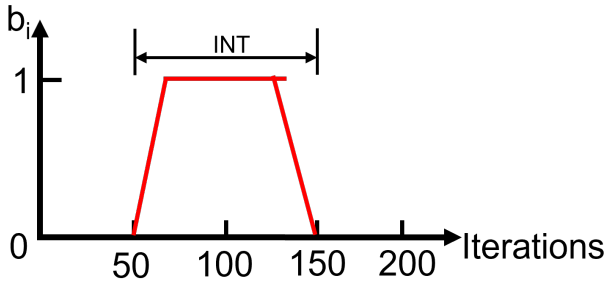

FIGURE 3.5: Progression of b_i over the iterations

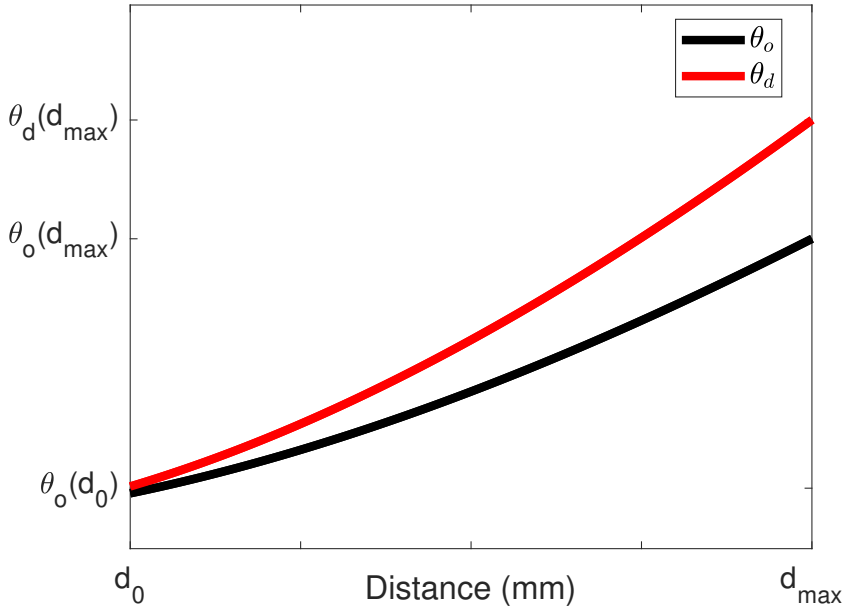

FIGURE 3.6: Desired swivel angle θ_d (see Equation 3.3) over reaching distance in ISC: the black solid line an example of θ_o (in PRE); the red solid line the corresponding θ_d in the Intervention phase

3.1.5 Experimental protocol

The protocol was divided into three successive phases[1] detailed below and summarized in Table 3.1.

TABLE 3.1: Experimental protocol

Phase	Free	PRE	INT	POST	Free
Force field	N.A.	Transparent	ISC	Transparent	N.A.
Iterations	1-25	26-50	51-150	151-175	176-200

[1]Two additional phases of 25 reaching tasks each without the robotic device where also performed prior and after these three phases and are not analysed here.

1. PRE phase, where subjects performed 25 reaching tasks while strapped to the robot. In this phase, the robot is set in transparent mode, compensating only for its own weight and friction in both vertical and planar directions, in order to minimise its influence on the subject. The movements recorded in this phase are used to obtain a reference for each subject.

2. INTervention phase, where subjects remained strapped to the robot and performed 100 reaching tasks. The robot applied the "ISC mode" in addition to its own gravity and friction compensation.

3. POST phase, identical to the PRE phase, where subjects performed 25 reaching tasks with the robot set in transparent mode. This phase was included to measure the washout effect.

4. FREE phase, where subjects performed 25 reaching tasks without the robotic device prior and after these three phases.

Subjects performed a total of 200 movements (including 50 movements in free phase, see Table 3.1). In order to reduce the potential influence of muscle fatigue, subjects were asked to take at least a thirty-second break every 20 iterations and could request additional rest at any time.

Subjects were not given any instruction about the different phases of the experiment and were blind to the objective of the experiment and to the effect of the robotic force field. Making the subjects unaware of the objective is required here to minimise to the best extent possible that no active or conscious behaviour is influencing the results.

At the end of the experiments, to test their awareness of the effect of the robotic device, all subjects were asked to take a questionnaire which consisted of the following questions:

- Question 1: Did you feel the robot applying any force?

- Question 2: Do you think the robot was influencing your movement in a particular way? If yes, what was that influence?
- Question 3: Do you think you changed the way you moved during the experiment? If yes, how did you change the way you move?

3.2 Results

Results are presented in three parts, respectively presenting the subject awareness of the robotic effect, the intervention effect and the after effect as measured by the change in swivel angle, and the change in hand velocity.

3.2.1 Questionnaire results

According to answers to the questionnaire, all of the subjects felt a force field was applied by the device (Q1). No subject suspected that the device influenced them in a particular way (Q2). All subjects did not feel that they changed their movement patterns (Q3).

3.2.2 Intervention outcome and after effect

To evaluate the effect of the intervention and after effect, the primary measure is the swivel angle change in the experiment. Only the angle at the end pose ($\theta\left(d_{max}\right)$) was used to represent the swivel angle of the movement in the analysis.

To investigate the true change of the swivel angle induced by the intervention as well as after effect in the POST phase, the average value $\theta_o(d_{max})$ recorded during the PRE phase for each subject was subtracted to the measures obtained in each subsequent phase. This swivel angle change was recorded as $\Delta\theta\left(d_{max}\right)$.

For each individuals, this average measure is thus reported:

- during the PRE phase, used as a baseline;
- during the INT phase (iterations $i = [66 - 135]$, in which without effect of b_i), to investigate the immediate effect of the ISC compared with baseline for each individuals;
- during the POST phase, to investigate the after effect of the ISC compared with baseline for each individuals.

The results are thus reported on intervention effect by comparing at group level with the mean swivel angles, $\theta\,(d_{max})$, of each individuals in PRE and INT phases using a Wilcoxon Signed-Rank Test [78].

Identically, the after effect is reported by comparing at group level with the mean swivel angles, $\theta\,(d_{max})$, of each individuals in PRE and POST phases using a Wilcoxon Signed-Rank Test.

The post-processing of the data and statistical analysis were performed using MATLAB 2019b (The MathWorks Inc., USA).

The changes of mean swivel angle during different phases for each individual subject is shown in Figure 3.7.

TABLE 3.2: Within-group comparisons for intervention effect and after effect

Phases	PRE-INT	PRE-POST
Difference	$+4.9°$	$-0.3°$
p value	0.002	0.6953
Test Statistic (W)	0	23

The evolution of $\Delta\theta\,(d_{max})$ is shown in Figure 3.8. The intervention effect is significant ($p = 0.002$), and the mean changes were $4.9°$ in INT phase as reported in Table 3.2. Additionally, a similar analysis performed not at end point, but midway through the movement (at $d = d_{max}/2$), shows a swivel angle increase of $1.9°$ confirming that the same trend exist through the reaching movement.

As the force field is progressively removed (from iteration 135), no after effect is observed, with a fast return to the baseline value. No significant differences

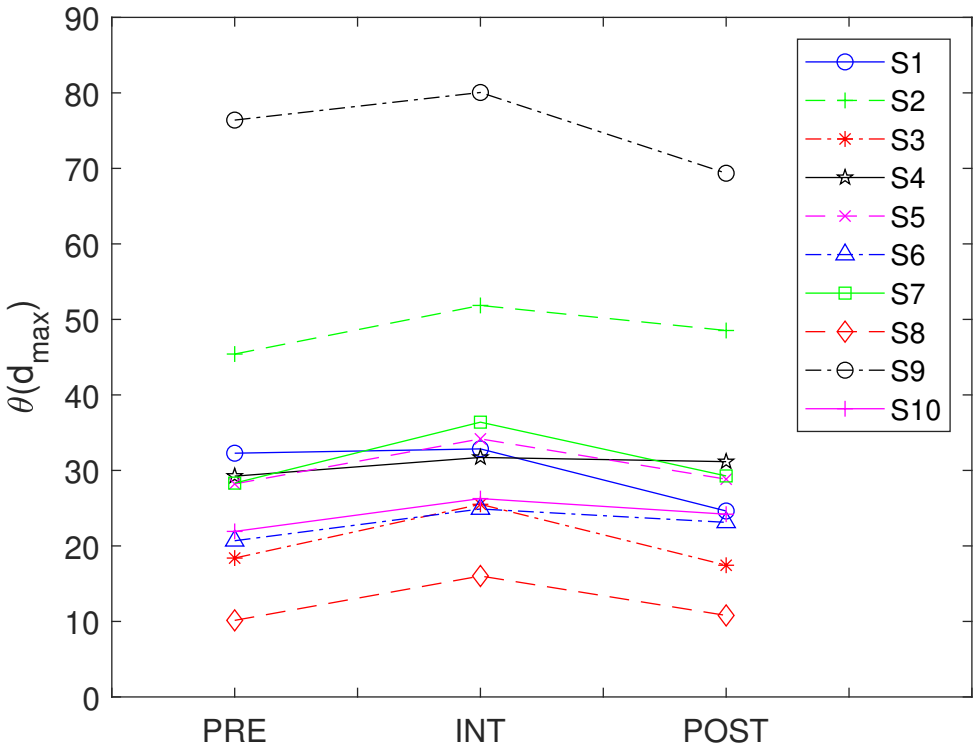

FIGURE 3.7: Mean swivel angle measure for each individual subject in the CG Group in the 3 phases of the experiment.

are found between PRE and POST phases ($p = 0.70$), with mean differences of $-0.3°$, as reported in Table 3.2. Figure 3.7 shows that this behaviour is relatively consistent among subjects, with only one individual not returning to their baseline behaviour (Subjects #9). Additionally, it can be seen on Figure 3.8 that subjects already started to return towards their baseline movement pattern during the phasing out of the force field (iterations 135 to 150).

3.2.3 Hand velocity

A secondary metric ϕ was introduced to evaluate the potential effect of the force field on subjects' movement "strategy". Indeed, given that the proposed additional movement cost introduced by the ISC is based on the movement velocity, a change in the velocity could explain a different optimisation from the subject to counteract this additional movement cost. The average velocities of each iteration,

$\overline{\|\dot{\mathbf{x}}^{\{PHASE\}}\|_2}$, were obtained after position differentiation, and the average over the different phases was then calculated. A coefficient of velocity change between PRE and comparative stage of INT phases was then obtained for each subject as:

$$\phi = \frac{\left(\overline{\|\dot{\mathbf{x}}^{INT}\|_2} - \overline{\|\dot{\mathbf{x}}^{PRE}\|_2}\right)}{\overline{\|\dot{\mathbf{x}}^{PRE}\|_2}}, \text{ where } \overline{\|\dot{\mathbf{x}}^{PRE}\|_2} \neq 0 \ . \tag{3.5}$$

Similar to the intervention outcome and after effect reported in Section 3.2.2, the hand velocity change is reported by comparing at group level with the mean values of ϕ of each individuals in PRE and INT phases using a Wilcoxon Signed-Rank Test.

The velocity change ratio ϕ (defined in Equation 3.5) is shown on Figure 3.9. A reduction of the average hand velocity of 20% was observed in both the INT and POST phases.

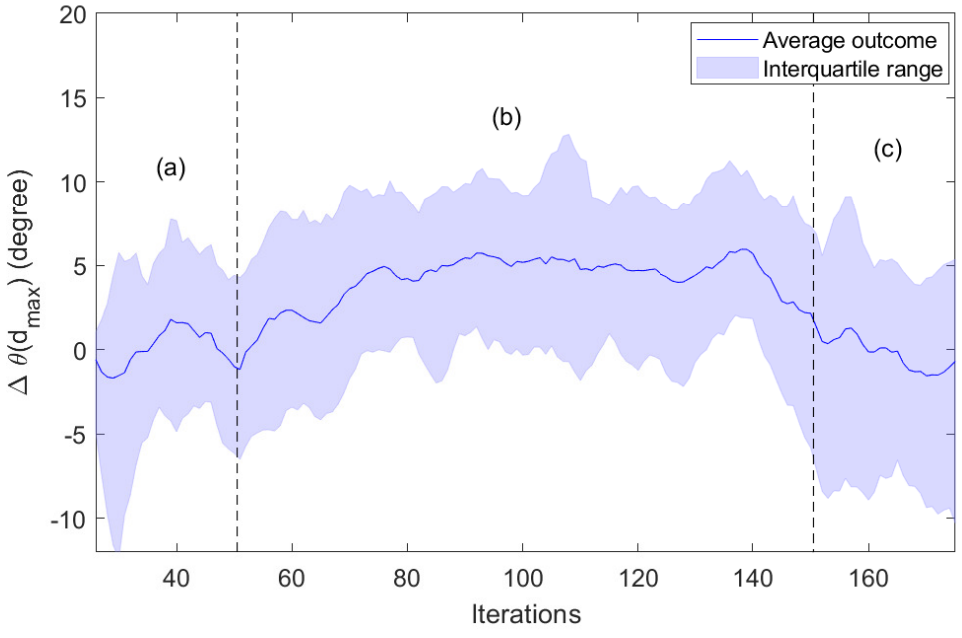

FIGURE 3.8: Swivel angle evolution for all subjects (sliding average with window width of 5 samples). The blue solid line shows the mean outcome in each iteration for all subjects. Shaded areas represent the interquartile range after rejecting outliers (three-sigma rule). Dotted lines shows the different phases: (a): PRE phase, (b): INT phase, (c): POST phase.

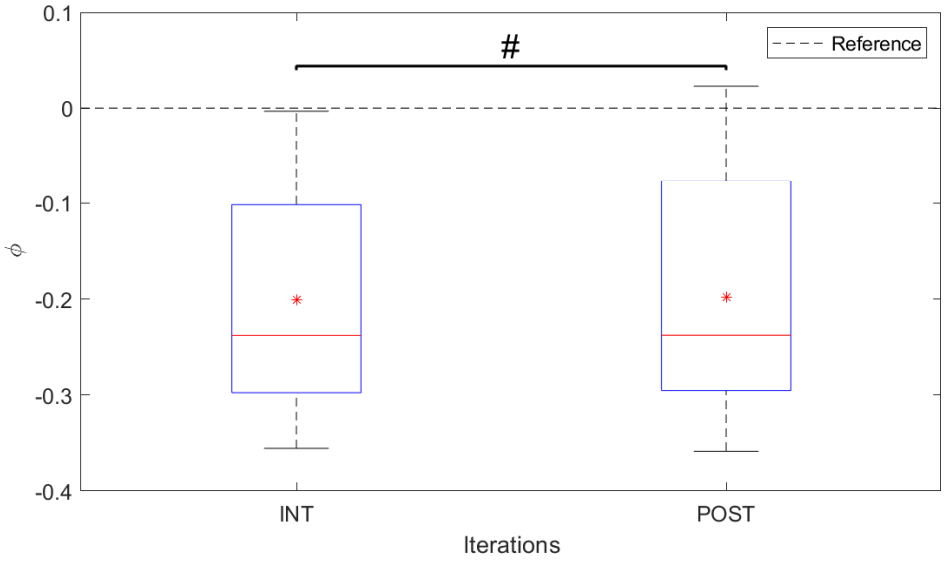

FIGURE 3.9: Velocity changes ratio. The box plot shows velocity changes ratio ϕ in the INT and POST phases. The bottom and top edges of the blue box indicate the 25th and 75th percentiles respectively while the red + shows the outliers. Inside the blue box, the red solid line shows the median and the red star shows the mean value of the data set. #: $p \geq 0.05$.

3.3 Discussion

3.3.1 Effects of ISC

A significant change in movement pattern was observed per their swivel angle in the INT phase. Although the changes remain of relatively small amplitude (4.9°) this demonstrates the possibility that motor behaviour can be influenced in a desired "direction" (*i.e.* an increase of the reaching swivel angle) without direct physical intervention and without explicit instructions given to the subjects. The observed adaptation is thus happening in the absence of any kinematic error, as it is purely dependant on the arm-null space kinematic and completely implicit (no subject realised the objective of the force field). This suggests that implementation of force field solely based on an artificially designed optimum can lead to an adaptation.

In [52], Izawa et al. stated that "[...] motor control in a novel environment is not a process of perturbation cancellation. Rather, the process resembles reoptimization: through practice in the novel environment, we learn internal models

that predict sensory consequences of motor commands." In their view, the goal of adaptation is not to cancel the error but to maximize performance in that environment. In their study, they showed that in a velocity-dependent force field that perturbs the hand orthogonally to the direction of a reaching movement, the human would adapt their reaching trajectory in a curved path and not a straight line to maximize the performance. And when the force field becomes stochastic (changing from trial to trial), the path plan could be reoptimized and take into account this uncertainty. Similar adaptation is observed in a 3D force field in this experiment — the adaptation of the subjects to the indirect force field falls within the reoptimization described by Izawa et al. [52]. In this study, the novel environment was made of an indirect force field altering the effort space, and subjects did explore this effort space and reoptimize their behaviour accordingly.

It is important to note that every subject demonstrated a change in the expected "direction". These results strengthen the ISC approach introduced by Fong in [76] where limited results were presented. The initial experiment and this study shared the same apparatus and setup but with two differences which may explain the different results. The first change is that in the previous work, the velocity measurement and physical contact point were at the center of the wrist. The present work changed this to the center of the hand. Thus, the previous version potentially prevented a fully free movement around the swivel angle for the subjects, due to this physical constraint at the wrist. The second change is the measurement of θ_o which is here modeled as a polynomial instead of taken as a linear relationship on constant mean value in the previous work. Thus, the previous work may have led to a more artificial linear swivel angle change along the trajectory, while the current implementation better respects the natural movement pattern reference along the path, only influencing a shift of this value.

No after effect can be observed, suggesting that the subjects quickly came back to their original movement pattern when the force field was removed. Despite the application of an implicit approach, supposedly leading to better retention [59], in this study, after effect was not expected to happen, as the desired exaggerated new

movement pattern leads to a higher cost when the robotic force field is removed, due to the existence of gravity. Subjects thus do not gain any benefit from this new movement pattern when they are moving without the artificial force field.

This minimal after effect differs from the results observed by Proietti et al. where a direct, but implicit, movement shaping is provided with an exoskeleton [5]. In their work, a direct torque was applied on the corresponding joints to shape the joints' coordination. The retention observed in their experiment could be due to the larger effect observed on their subjects at the end of the INTervention phase, leading to a longer washout.

Additionally, in [5], the subjects' awareness was not checked after the experiment making it difficult to fully conclude on whether the subjects voluntarily adapted to the force field, or were conditioned to move in a certain way when placed in the test setup.

3.3.2 Motor cost compromise

In ISC, the artificial additional cost introduced is in the form of a viscous force opposed to the movements in the direction of the hand's velocity, with a higher velocity causing higher viscous force magnitude. The viscous force field is proportional to both swivel angle error and velocity (as per Equation 3.4) and the subjects could thus choose to comply to the swivel angle requirement, to reduce their reaching velocity, or a combination of both, in order to reduce the intensity of the force field. In Figure 3.9, it can be clearly seen that subjects slightly reduced their velocity magnitude to avoid the resistance in completing the task in the majority of iterations.

Due to the nature of the task, the natural motor cost is here dominated by the gravitational load, which is static by essence: a higher swivel angle will lead to a larger load on shoulder muscles for a given posture. A slower movement will require additional energy, as the load will have to be sustained for a longer time.

But limiting the speed of movement could reduce the movement cost from robotic device which is velocity dependent. The cost introduced by the ISC thus counteracts this effect and a compromise between these two costs is expected to be found by the subjects. This can explain the reduction in the hand velocity and the compliance of the subjects to the modification of their swivel angle, suggesting an exploration of the cost space by the subjects.

Additionally, it could be seen that the average swivel angle "reached" by all subjects is below the shaping goal at which the artificial component in the cost function could become zero, also suggesting a cost trade-off between the gravitation and the artificial force field.

3.3.3 Subject awareness

From the questionnaire results, the subject awareness can be evaluated. All participants were asked to focus on finishing the quiz and reaching tasks. As all participants did not realize either the actual effect of the robotic device or their movement pattern change, the training can be seen as truly implicit.

It is important to note that here the healthy subjects are physically easily capable of complying with the objective. If the subjects were explicitly described the desired movement pattern as well as the study objective, the results would be affected by how much the subjects want to cooperate with the researchers. In fact, the implicit learning approach, even if suspected to lead to better retention, may not be possible or practical in a neuro-rehabilitation context where subjects may have little movement variability of movement to even explore the cost, and thus comply to it [79]. In any case, if the shaping component of the training is left implicit, it is important, as suggested in [5] to keep another reward mechanism. This mechanism can be task, and not shaping, related and classically in the form of gaming and/or a score to ensure motivation [80] as well as favour dopamine release to promote brain plasticity [81].

3.3.4 Translation to neuro-rehabilitation

The chosen task and problem in this study aims to be relevant to motor neuro-rehabilitation of the upper-limb, where pathological synergies retraining and movement correction play an important role towards functional recovery. This study aimed to provide a method in adapting human's movement pattern by adding an indirect force field. The results demonstrate the feasibility of changing the joint space coordination by using a manipulandum device by adding an artificial task space cost. Indeed, compared to the previous work using exoskeletons [4, 5], this approach allows the use of much simpler and accessible devices for the same objective. But despite cost and practicality, the indirect approach could also have the additional benefit of actually requiring the subjects to completely adopt the movement pattern by not directly physically constraining it. The effect that is observed in the redundant space to be shaped is purely driven by the subjects, and not a combination of the robotic and the subject inputs as in the case with the KSC implementation [82].

A similar setting to ISC, using a force resistance at the hand as a function of trunk compensations has also shown some positive effect in reducing compensatory movements with individuals with hemiplegia [74]. The effect was shown to be larger than classically using trunk restraint which suggests a possible translation of our proposed method to this application with the opportunity to generalise it to more complex movement pattern correction.

3.4 Summary

Indirect Shaping Control (ISC) is an approach to influence redundant space movement patterns indirectly and implicitly based only on cost/effort applied in task space. The experimental validation results show that all subjects but one did adapt their movements towards the desired movement pattern (as measured by

the swivel angle) when trained using the robotic manipulandum, but no after effect was observed. These results extend the previous preliminary conclusions on such an approach and suggest that an alteration of movement patterns using an indirect motor cost approach is feasible. It would be expected that retention might be observed only at the condition that the learned movement pattern provides an actual follow-up benefit to the subjects. Although all but one subjects adapted their movements, the average change was only around 5°. To improve this limited outcome, a new variation of ISC will be introduced in the next chapter.

Chapter 4

Contribution of progressivity in indirect shaping control

In Chapter 3, a constant goal was set during the intervention phase to induce an indirect movement pattern change. Given this change fully relies on the change of motor cost induced by an artificial force field, it may be difficult for the subjects to find the optimum with an implicit and indirect method. Assuming that this adaptation may be further promoted through subtle prompts to explore the cost space, a variation of the approach with a progressive goal could be potentially helpful. A progressively changing goal is usually used to improve one's capabilities gradually when the limits of those capabilities are unknown. Examples of such an approach can be seen in neuro-rehabilitation, where recovery is not achieved suddenly but rather progressively [20, 21]. Exercises and tasks are thus defined progressively to encourage motor control changes. In this process, clinicians usually set a reachable goal and move it further and further to favour changes. This applies either to practiced tasks of increasing difficulties (*e.g.* Range of Motion or finer motor control) but also to the expected changes in motor behaviours (movement quality, limitation of over-recruitment, movement smoothness or movement speed).

This progressively changing goal takes its theoretical basis in physiology. Neuroplasticity studies show that the changes in neural configuration can happen only

when the inputs to the neurons circuitry — and so the learning steps — falls within their anatomical available resources. This thus limits the learnable step-size but does not ultimately prevent large scale changes if they are presented progressively [81]. The brain physiology studies show that exposing to a progressively changing environment, the primary midbrain source of noradrenaline is enduringly up-regulated, which resulted in the increase of the baseline level of excitability in the cortex. And it can positively amplify the plastic change [83–85]. In this case, the repetition and overlap in training are necessary to achieve the optimizations. Based on this principle a new variation of ISC is designed and presented in this chapter.

4.1 A new variation of ISC

The general idea of this ISC was still a viscous field applied to the subject's hand movement as a function of the current swivel angle value. The viscous force field followed the same algorithm as introduced in Equation 3.3 and Equation 3.4. The main difference between these two variations of ISC was that $\theta_{goal}(i)$ was set to a constant value across all iterations in the intervention in the previous experiment and linearly increased from 0 to $\theta_{goal}(i)$ in the first half of the intervention and kept constant at $\theta_{goal}(i)$ for the second half of intervention (see Figure 4.1). To differentiate these two different variations, the ISC applied in the previous experiment is named Constant-ISC (C-ISC), and the experiment results are presented as Constant Goal (CG) Group. The new variation of ISC is now named Progressive-ISC (P-ISC), and the corresponding subjects and results are in Progressive Goal (PG) Group.

4.2 Experimental validation

Here, a new hypothesis that a progressive goal would lead to a larger movement pattern modification than a constant goal will be tested. The new test group

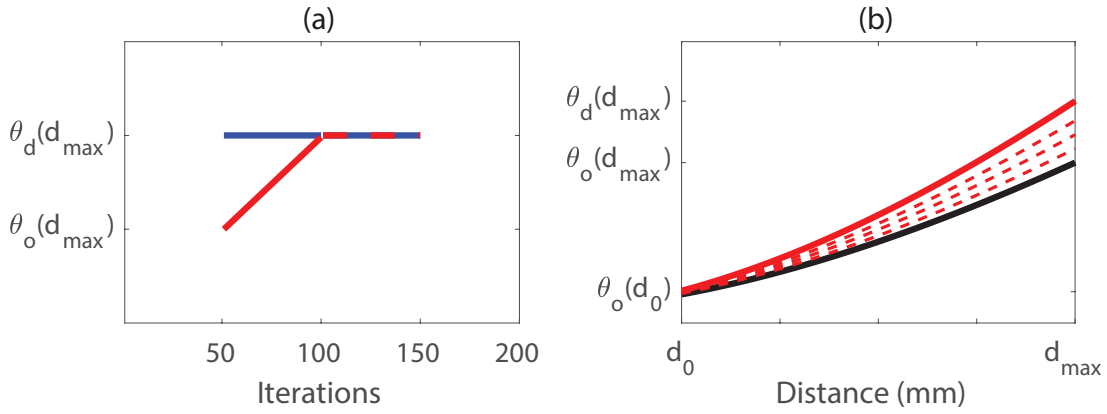

FIGURE 4.1: (a): Desired swivel angle θ_d (see Equation 3.3) at the end pose ($d = d_{max}$) over iterations for C-ISC and P-ISC. (b): desired swivel angle θ_d over reaching distance for C-ISC and P-ISC with: the black solid line an example of θ_o (in PRE); the red solid line the corresponding θ_d for the second half of the INTervention applied in the Progressive Group and the entire INTervention phase applied in the CG Group; and the red dashed lines examples of intermediate θ_d in the first half of INTervention phase in the PG Group.

(PG Group) shares the same experiment setup except for the shaping goal of the force field, which was a constant number of 10° in the previous group (CG Group) and a progressively changing goal in PG Group. Thus, the results presented in Chapter 3 can be a control group results to compare with the results collected in this group. A consistent evaluation of two variations of the ISC is thus performed where the force field encourages a change in the redundant space without any explicit instruction nor direct physical effect in the adaptation space.

Note that θ_{goal} was the same (10°) for both groups in the second half of the intervention and that b_i function was used in both groups for consistency and to avoid to raise subject's awareness at the removal of the force field.

4.2.1 Participants

As multiple tests may influence the consciousness on the objective of this experiment, to keep the experiment in a fully implicit manner, ten new subjects were invited. Five female and five male subjects (age: 24.2 ± 1.7) participated in this experiment. All of these subjects were right-handed and did not suffer from any impairment in their upper-limb motor functions in past two years.

This experiment was approved by the University of Melbourne Human Research Ethics Committee (#1749444), and an informed written consent was received from all subjects.

4.2.2 Task design

This experiment shares the same task design as the previous experiment. The objective of the robotic intervention was to increase the swivel angle (see θ on Figure 3.2) with which the subject was performing reaching tasks using his/her dominant hand. Participants were required to sit on a fixed chair and repeat a reaching movement. During the experiment, the same quiz game was designed to distract the subjects from the exact objective of the study. No time limitation nor timing instructions were imposed to participants who were performing the reaching task at their own comfortable pace. Detailed task design was presented in Section 3.1.2.

4.2.3 Apparatus and measurements

Compared to the previous experiment, the same apparatus and measurements were used in this experiment (see Section 3.1.3 and Figure 3.1). The EMU was used to generate the ISC force field while the subject's hand was attached to the handle of the device. TrakSTAR 3D Guidance Magnetic Sensors was used to measure the subjects' shoulder (S), wrist (W) and elbow (E) positions, which was subsequently used to calculate online the swivel angle as shown in Equation 3.1 and Equation 3.2.

4.2.4 Experimental protocol for variant of ISC

Identical to the previous experiment, the protocol was divided into three successive phases. The difference is that the force field applied in the Intervention was P-ISC

as shown in Table 4.1.

1. PRE phase, where subjects performed 25 reaching tasks while strapped to the robot. In this phase, the robot is set in transparent mode, compensating only for its own weight and friction in both vertical and planar directions, in order to minimise its influence on the subject. The movements recorded in this phase are used to obtain a reference for each subject.

2. INTervention phase, where subjects remained strapped to the robot and performed 100 reaching tasks. The robot applied the "P-ISC mode" in addition to its own gravity and friction compensation.

3. POST phase, identical to the PRE phase, where subjects performed 25 reaching tasks with the robot set in transparent mode. This phase was included to measure the washout effect.

Same as the previous experiment, subjects performed a total of 200 movements and were asked to take at least a thirty-second break every 20 iterations and could request additional rest at any time. The experiment was run in an implicit manner and the subjects were not given any instruction about the different phases of the experiment and were blind to the objective of the experiment and to the effect of the robotic force field.

The same questionnaire was taken by all subjects in this experiment at the end of the experiments to test their awareness of the effect of the robotic device.

TABLE 4.1: Experimental protocol for variant of ISC

Phase	Free	PRE	INT	POST	Free
Force field	N.A.	Transparent	P-ISC	Transparent	N.A.
Iterations	1-25	26-50	51-150	151-175	176-200

4.3 Results

To compare the outcome from two experiments and evaluate the contributions of the progressivity in this experiment, part of the results from previous experiment (noted as "CG Group") are also included. Results are presented in four parts, respectively presenting the subject awareness of the robotic effect, the within-group comparisons on the intervention effect and the after effect as measured by the change in swivel angle, the between-group comparisons on the difference between the two groups in altering subject's movement, and the change in hand velocity. Consistent data analysis of two variations of the ISC were performed in this and previous experiment.

4.3.1 Questionnaire results

According to answers to the questionnaire, all of the subjects in PG group felt a force field was applied by the device (Q1). Only one subject (1/10) in PG group suspected that the device influenced them in a particular way but was incapable of describing the actual effect (Q2). This subject also pointed out that he felt he changed his movement to "a parabolic trajectory" during the experiment, whereas all the other subjects did not feel that they changed their movement patterns (Q3).

4.3.2 Intervention outcome and after effect

The swivel angle at the end pose ($\theta\left(d_{max}\right)$) was used to represent the swivel angle of the movement in the analysis. And the swivel angle change was recorded as $\Delta\theta\left(d_{max}\right)$ as introduced in Section 3.2.2. For each individuals, this average measure is thus reported:

- during the PRE phase, used as a baseline;
- during the comparative stage of INT phase (iterations $i = [101 - 135]$, in which both groups share the same shaping goal without effect of b_i), to

investigate the immediate effect of the ISC compared with baseline for each individuals;

- during the POST phase, to investigate the after effect of the ISC compared with baseline for each individuals.

The results are thus reported on intervention effect by performing within-group comparisons on the mean swivel angles, $\theta\,(d_{max})$, of each individuals in PRE and comparative stage in INT phases using a Wilcoxon Signed-Rank Test for each group.

Identically, the after effect is reported by by performing within-group comparisons on the mean swivel angles, $\theta\,(d_{max})$, of each individuals in PRE and POST phases using a Wilcoxon Signed-Rank Test for each group.

The changes of mean swivel angle during different phases for each individual subject in PG Group are shown in Figure 4.2.

The evolution of $\Delta\theta\,(d_{max})$ for each group is shown in Figure 4.3. The intervention effect is significant for both groups ($p = 0.002$), and the mean changes were 4.9° and 6.3° in comparative stage of INT phase for CG Group and PG Group respectively, as reported in Table 4.2. Additionally, a similar analysis performed not at end point, but midway through the movement (at $d = d_{max}/2$), shows a swivel angle increase of 1.9° and 2.1° for CG and PG groups respectively, confirming that the same trend exist through the reaching movement.

As the force field is progressively removed (from iteration 135), no after effect is observed, with a fast return to the baseline value. No significant differences are

TABLE 4.2: Within-group comparisons for intervention effect and after effect

Group	CG (N=10)		PG (N=10)	
Phases	PRE-INT	PRE-POST	PRE-INT	PRE-POST
Difference	+4.9°	−0.3°	+6.3°	0.9°
p value	0.002	0.6953	0.002	0.7695
Test Statistic (W)	0	23	0	24

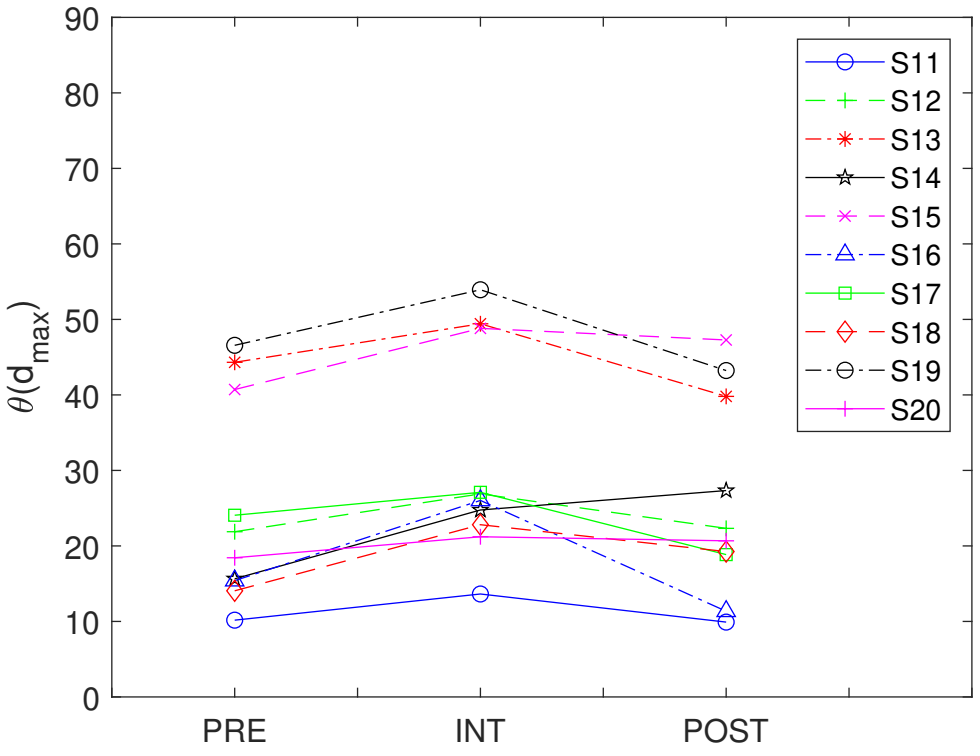

FIGURE 4.2: Mean swivel angle measure for each individual subject in the PG Group in the 3 phases of the experiment.

found between PRE and POST phases ($p = 0.70$ and $p = 0.77$ respectively for CG and PG Groups), with mean differences of $-0.3°$ and $0.9°$, as reported in Table 4.2. Figure 3.7 and 4.2 show that this behaviour is relatively consistent among subjects, with only a few individuals not returning to their baseline behaviour (Subjects #9, #14, #15 and #18). Additionally, it can be seen on Figure 4.3 that subjects already started to return towards their baseline movement pattern during the phasing out of the force-field (iterations 135 to 150).

4.3.3 Contribution of the constant and progressive goal

To compare the two variations of the ISC, the means of $\Delta\theta\,(d_{max})$ of each individual during the comparative stage of INT phase (iterations $i = [101 - 135]$) were further compared between groups using the Wilcoxon Rank-Sum tests.

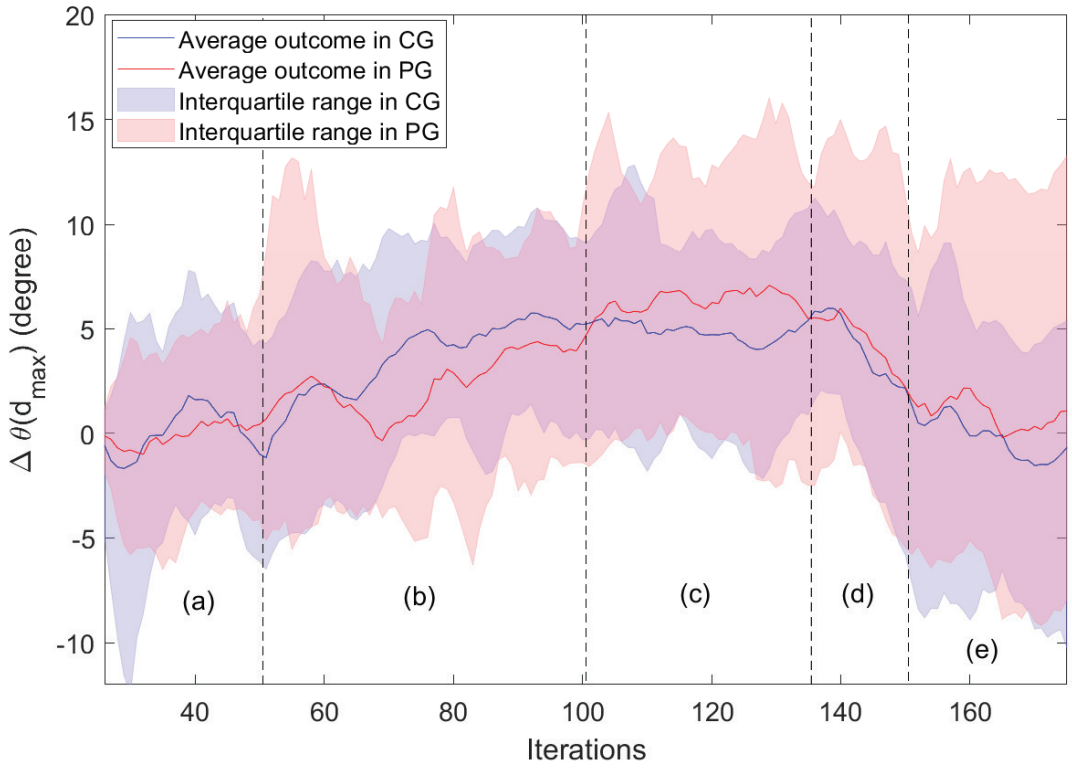

FIGURE 4.3: Swivel angle evolution for all subjects in each group (sliding average with window width of 5 samples). The blue and red solid line show the mean outcome in each iteration for all subjects in CG Group and PG Group respectively. Shaded areas represent the interquartile range after rejecting outliers (three-sigma rule). Dotted lines shows the different phases: (a): PRE, (b):first part of INT with progressive goal in PG, (c): comparative stage of INT with constant goal in both CG and PG Group, (d): progressive removal of force field, and (e): POST phase.

Figure 4.4 shows the change of swivel angle in the two groups during the comparative stage of INT phase compared to baseline (PRE). The difference between the two groups is small, at 1.4° and found to be not statistically significant (see Table 4.3).

TABLE 4.3: Between-group comparisons for intervention effect and after effect

Phases	INT	POST
Difference	1.4°	1.2°
p value	0.2730	0.9698
Test Statistic (W)	90	104

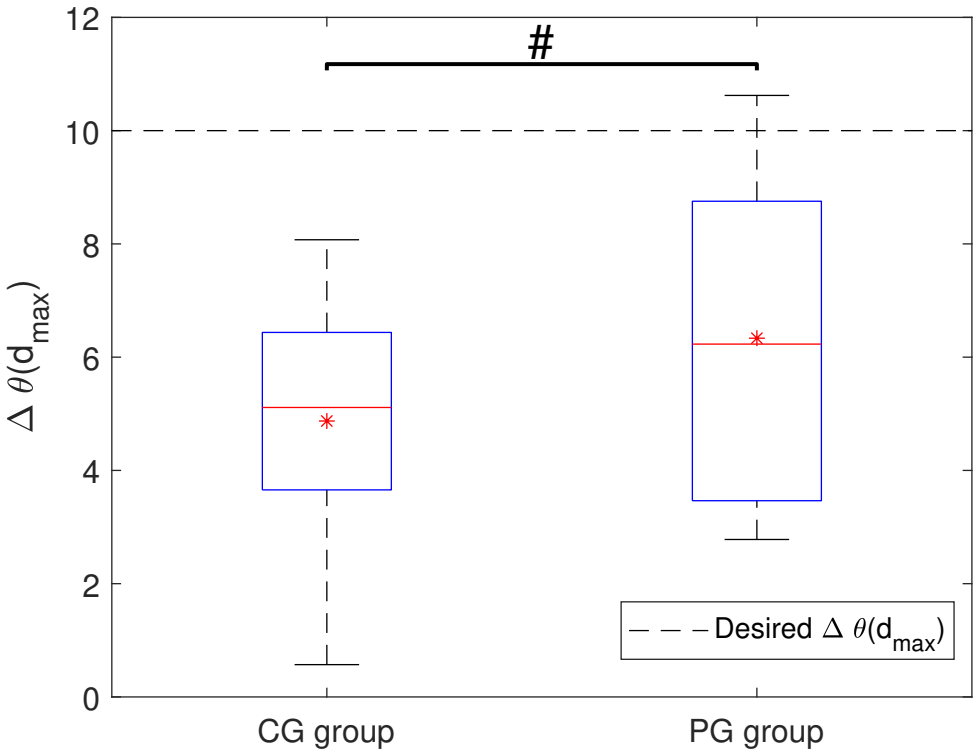

FIGURE 4.4: Swivel angle changes compared to baseline for each group. The box plot shows swivel angle changes $\Delta\theta\,(d_{max})$ in the comparative stage of INT for CG Group and PG Group respectively. The bottom and top edges of the blue box indicate the 25th and 75th percentiles respectively while the red + shows the outliers. Inside the blue box, the red solid line shows the median and the red star shows the mean value of the data set. #: $p \geq 0.0025$.

4.3.4 Hand velocity

Identical to previous experiment, the hand velocity changing ratio, ϕ (see Equation 3.5), was introduced to analyze the hand velocity changes. As for the swivel angle, the effect of the intervention on the hand velocity was assessed by comparing the INT and POST phases for each group, and between-group comparisons were performed to assess the effect difference of the two variations of the ISC. Within-group comparisons were tested using the Wilcoxon Signed-Rank tests, while Between-group comparisons were tested using the Wilcoxon Rank-Sum tests.

The velocity change ratio ϕ (defined in Equation 3.5) for each group is shown on Figure 4.5. A reduction of the average hand velocity of 20% and 16% was observed

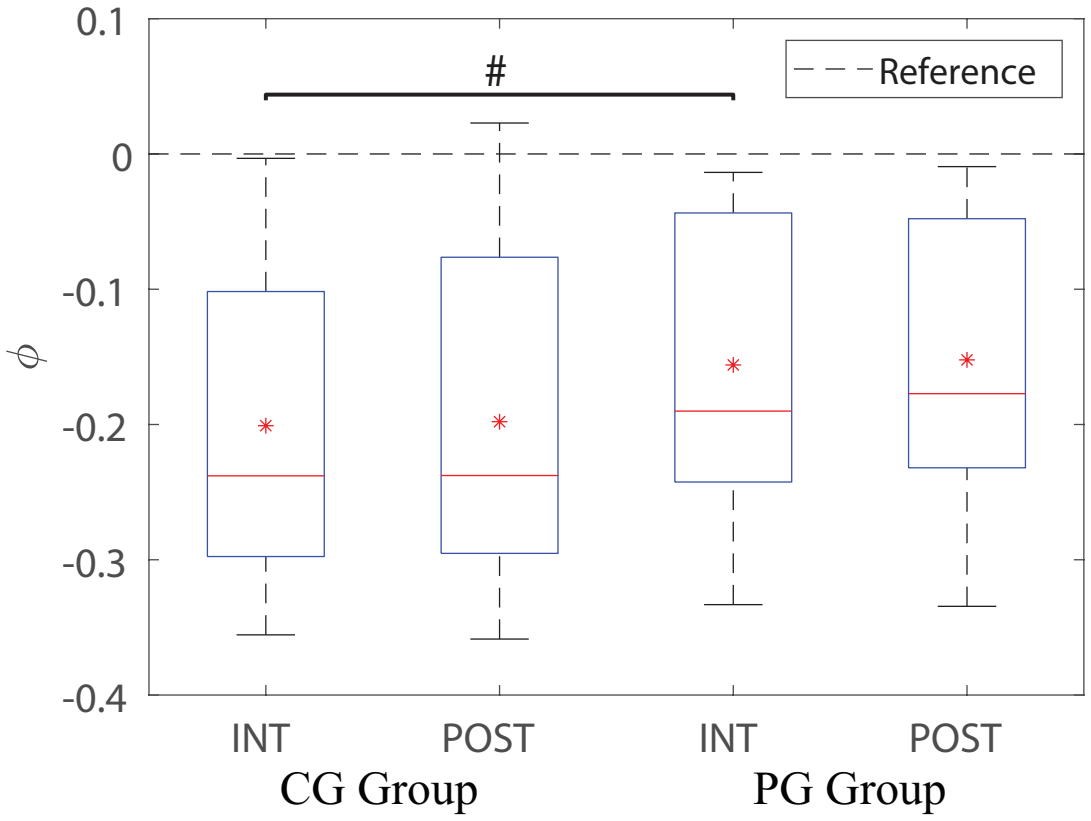

FIGURE 4.5: Velocity changes ratio for each group. The box plot shows velocity changes ratio ϕ in the comparative stage of INT and POST for CG Group and PG Group respectively. The bottom and top edges of the blue box indicate the 25th and 75th percentiles respectively while the red + shows the outliers. Inside the blue box, the red solid line shows the median and the red star shows the mean value of the data set. #: $p \geq 0.05$.

for the CG Group and the PG Group respectively in both the comparative stage of INT and POST phases. The difference between the two groups, 4%, was shown to be not significant ($W = 95$, $p = 0.4727$) as shown in Table 4.5. Similar results were observed for the within-group comparisons, and the difference was found to be not significant (see Table 4.4).

TABLE 4.4: Within-group comparisons for velocity changes in INT-POST

Group	CG (N=10)	PG (N=10)
Phase	INT-POST	
Difference	−0.3%	−0.4%
p value	0.695	0.922
Test Statistic (W)	23	26

TABLE 4.5: Between-Group comparisons for velocity change in PRE-INT and PRE-POST

Phases	PRE-INT	PRE-POST
Difference	4.5%	4.6%
p value	0.473	0.473
Test Statistic (W)	95	95

4.4 Discussion

4.4.1 Contribution of the progressive goal

Similar results were observed in PG Group compared to CG Group. A significant change in movement pattern was observed in both groups per their swivel angle in the comparative stage of INT phase (4.9° and 6.3° for the CG and PG respectively) and no after effect can be observed in either group. This result confirmed the possibility that motor behaviour can be adapted with the implementation of force field solely based on an artificially designed optimum.

In the specific case of our approach only relying on an artificial change of the motor cost, without any corresponding kinematic error, it was expected that this progressivity would assist the subject exploration of the cost space by making the minimal cost point more accessible at every step by ideally falling within the subject's natural variability.

The progressive goal approach evaluated here is shown to be slightly more effective in this context than its equivalent with a constant goal. The difference in outcome is of 1.4° which corresponds to an improvement of 29%. Similarly a difference in the effect can be observed from the swivel angle evolution over the iterations (see Figure 4.3). It can be seen in the comparative stage of INT phase that the PG Group has higher mean change in all iterations. However, this difference is not statistically significant and no concrete conclusion can be drawn on the advantage of this progressivity.

The progressivity defined in this experiment was a linearly changing goal. It can be seen that the shaping outcomes varied from person to person. This suggests that adding personalised force-field could potentially contribute to enhance the contribution of this progressivity. For example, slower or pausing the movement of the goal when trainees are not able to achieve it. In clinical application, this personalisation is common, as clinicians usually offer different treatments to different patients in different stages. However, if personalised feedback is integrated into ISC, it is important to ensure that this less challenging goal does not induce slacking which may reduce human effort during rehabilitation training and cause significant reduction in the outcome of the shaping [86].

4.4.2 Subject awareness

The overall results from questionnaire are similar to the previous experiment. As all participants could not describe the actual effect after experiment, the training can be seen as truly implicit.

A special case among them is Subject 14 who pointed out that a change of his movement pattern occurred during the experiment, and whose shaping outcome is one of the largest observed across the subjects (9.15°, see Figure 4.2). It is to note that this subject has significant larger variations of their swivel angle than other subject during the comparative stage of the INT phase. This variation shows a larger exploration of the cost space and potentially demonstrates that the subject noticed the force field and explicitly changed their movement pattern during the experiment. Interestingly, even though the subject was not able to describe the actual intervention effect, they still found the way to reduce the movement cost by complying to the desired movement pattern.

4.5 Summary

This study confirmed the feasibility of shaping human movement patterns indirectly and implicitly by relying on the motor cost change only. However, the contribution of progressivity is not significant in the current experimental setup. In the current setup, the progressivity is the same static trend for all subjects, but in actual clinical therapy, the progressivity is usually personalized based on each subject. A guessing is thus proposed that progressively moving the goal based on individual learning outcome could be a better solution. This personalized moving goal could potentially better interpret the principle on neuroplasticity. As the same task was chosen in this experiment, retention is still neither expected nor observed. To better understanding the observations from these experiments, a motor cost analysis is performed and presented in the next chapter.

Chapter 5

Motor cost analysis

The previous chapters have confirmed that motor adaptation can be induced with an indirect and implicit method which relies on the motor cost change. In this chapter, a more specific analysis of how the motor cost changes during the experiment is presented. This analysis aims to explain the observations from the experiment and also validate the conjecture of the relationship among swivel angle, velocity, and motor cost mentioned in previous chapters.

As introduced in Section 2.1, different models have been proposed to estimate the motor cost, based on different formulations of the cost function. Among three types of cost functions indicated in Section 2.1, the cost function based on kinematic parameters (*i.e.* jerk of the hand movement [24] or swivel angle [25]) has its advantages due to its simplicity of the observations, but it cannot explain all scenarios in human's daily life. For example, putting a bottle with and without water onto a table can lead to a different motor cost. This example shows that the cost function for dynamic systems can be parameterized by some parameters to characterize the dynamics at either mechanical level [26–28] or neuorological level [29, 30, 34] (see detailed descriptions in Section 2.1). These cost functions can provide more detailed information compared with cost function based on kinematics only.

As there is no neurological signal measured in the experiment, the cost function based on the parameters of mechanical dynamics parameters is chosen. In this chapter, the human arm model will be simplified to a two-link mechanism and to illustrate the motor cost compromise in this experiment. The motor cost will be estimated based on the Torque-Time-Integral (TTI), which can reflect the energy expenditure during the movement [87]. Although this model cannot precisely describe the real motor cost change during the experiment, it can still contribute to understanding the strategies that subjects made in the experiment.

5.1 Computational model and cost function

This subsection will discuss the model and the cost function that are employed in building the computational model.

5.1.1 Arm kinematics model

To analyze the motor cost change, the human arm was simplified as a two-link mechanism with a ball joint (or equivalent three revolute joints) for the shoulder and a revolute joint for the elbow, with two point masses m_1 and m_2 representing the upper arm and forearm respectively, as shown in Figure 5.1. The length of the links are set to l_1 and l_2.

Labelling the four joints with q_1, q_2, q_3 and q_4, among which q_1 represents the shoulder internal/external rotation, q_2 represents the shoulder extension/flexion, q_3 represents the shoulder abduction/adduction, and q_4 represents the elbow extension/flexion. Through the forward kinematics model, the relationship between the joint space and the task space can be represented as

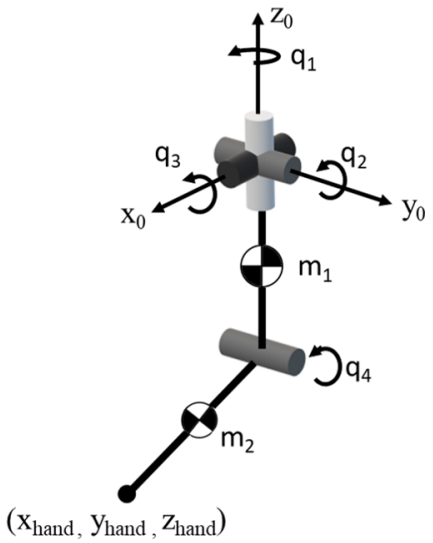

FIGURE 5.1: The arm model used for the cost simulation with four revolute joints and two mass centered on the two links.

$$\begin{aligned} x_{hand} =& l_1(\cos q_2 \cos q_1 + \sin q_2 \sin q_1 \sin q_1) \\ &+ l_2(\cos q_4(\cos q_2 \cos q_1 + \sin q_2 \sin q_1 \sin q_1) \\ &- \sin q_4(\cos q_2 \sin q_1 - \cos q_1 \sin q_2 \sin q_1)). \end{aligned} \tag{5.1}$$

$$\begin{aligned} y_{hand} =& l_2(\cos q_1 \cos q_1 \sin q_4 + \cos q_1 \cos q_4 \sin q_1) \\ &+ l_1 \cos q_1 \sin q_1. \end{aligned} \tag{5.2}$$

$$\begin{aligned} z_{hand} =& - l_1(\cos q_1 \sin q_2 - \cos q_2 \sin q_1 \sin q_1) \\ &- l_2(\cos q_4(\cos q_1 \sin q_2 - \cos q_2 \sin q_1 \sin q_1) \\ &- \sin q_4(\sin q_2 \sin q_1 + \cos q_2 \cos q_1 \sin q_1)). \end{aligned} \tag{5.3}$$

As shown in Equation 5.1 to Equation 5.3, with the known hand position $(x_{hand}, y_{hand}, z_{hand})$, there are infinite sets of $\mathbf{q}_n = [q_1\ q_2\ q_3\ q_4]^{\mathrm{T}} \in \mathcal{R}^4$ value can be chosen, which reflects the redundancy of this model, and this redundancy can be

parametrised by the swivel angle θ. The relationship between swivel angle θ and joint angles $\mathbf{q}_n$ is

$$\theta = \arcsin\left(\cos q_1 \cos q_3 + \sin q_1 \sin q_2 \sin q_3\right). \tag{5.4}$$

Thus, for a known swivel angle as well as the hand position, $\mathbf{q}_n$ in joint space can be uniquely defined, thus, the redundancy is resolved.

With the equality constraint introduced in Equation 5.4, the measured task space movement can be uniquely mapped to the joint space to reflect joint changes. Consequently, the cost can be estimated based on the torque changes at each joint.

5.1.2 Arm dynamics model and cost estimation

The motor cost or energy consumption is estimated by using the Torque-Time Integral (TTI) [87], assuming that each joint has an equal contribution. The two main costs included in this analysis were the cost induced by the force field and the natural cost induced by gravity and kinetics.

The natural cost of the reaching task, $\mathcal{L}_n$ can thus be estimated as integral of the sum of the kinetic and gravity torques over time t:

$$\mathcal{L}_n = \int_0^T |\tau_{gravity}(t)| + |\tau_{kinetics}(t)| \ dt \ , \tag{5.5}$$

where $|\circ|$ denotes absolute value. If the measurements are sampled, the integral becomes a summation.

The total cost during the intervention phase, $\mathcal{L}_i$, as the integral of the sum of the natural cost $\mathcal{L}_n$ and the cost induced by the force field:

$$\mathcal{L}_i = \int_0^T |\tau_{gravity}(t)| + |\tau_{kinetics}(t)| + |\tau_{force-field}(t)| \ dt. \tag{5.6}$$

The gravity torque of the two links is computed as follows:

$$\tau_{gravity}(t) = \sum_{n=1}^{2} -\mathbf{J}_{C_i}(t)^T \cdot m_i g \cdot \mathbf{v}, \tag{5.7}$$

where $\mathbf{J}_{C_i}(t)$ is the Jacobian matrice to the respective centers of mass and $\mathbf{v}$ is the vertical vector $[0\ 0\ 1]^{\mathrm{T}}$. It is the torque due to gravity on both links of mass m_1 and m_2.

The kinetic torque of the two links is computed as follows:

$$\tau_{kinetics}(t) = \sum_{n=1}^{2} \left(m_i \cdot \mathbf{J}_{vC_i}(t)^T \cdot \mathbf{J}_{vC_i}(t) + \mathbf{J}_{\omega C_i}(t)^T \cdot \mathbf{I}_{C_i} \cdot \mathbf{J}_{\omega C_i}(t) \right) \cdot \ddot{\mathbf{q}}, \tag{5.8}$$

where $\mathbf{J}_{vC_i}(t)$ and $\mathbf{J}_{\omega C_i}(t)$ are the translational and rotational Jacobian matrices of the centers of mass respectively. The notion $\mathbf{I}_{C_i}$ is the inertia matrices of the two segments.

The torque induced by the force field is:

$$\tau_{force-field}(t) = \mathbf{J}_H(t)^T \cdot \mathbf{f}_{vis}(t). \tag{5.9}$$

where $\mathbf{J}_H(t)$ denotes the Jacobians to the hand point (H) and $\mathbf{f}_{vis}(t)$ is the viscous force field generated by the robot.

5.2 Motor cost simulation

Based on this kinematic model and the motor cost function, a simulation environment can be developed. With this simulation, it is expected to illustrate the relationships among the swivel angle, hand velocity and motor cost.

5.2.1 Simulated trajectories

The simulated trajectory was applied in the model to illustrate the movement pattern change associated with the corresponding cost change. The parameters and trajectories selected in this simulation correspond to the average of the measurement from the twenty subjects in the experiment. The linkage lengths are the average of the twenty subjects; namely, the lengths of the linkages are set to $l_1 = l_2 = 300$mm. The mass of the upper arm and forearm were set to $m_1 = 2.3$kg and $m_2 = 1.7$kg based on the average of the estimated segment weight using their body weight [88]. The starting and final points of the hand movements were $[305, -60, -400]mm$ and $[500, 110, 0]mm$ respectively based on the average trajectories of the experimental data. In this coordinate system, the positive x, positive y and positive z directions represent the forward, leftward and upward directions respectively.

The average velocity was set to $400mm.s^{-1}$. The original swivel angle trajectory θ_o was define with $\theta_o(0) = 15°$ (at the starting pose) and $\theta_o(d_{max}) = 25°$ (at the end pose) based on the average measurement in the experiment. The force field desired swivel angle was thus set to $\theta_d(d_{max}) = 35°$ (at the end pose), and the force field were calculated based on Equation 3.4.

5.2.2 Simulation results

The total most costs, $\mathcal{L}_i$, of the reaching movements estimated for variations of the swivel angle and hand movement speed are shown in Figure 5.2. The value of 0° swivel angle change and speed of $0.40m.s^{-1}$ corresponds to the average movement in PRE phase. The speed ranges are ±10% and ±20% of the average speed, while 10° swivel angle change is the desired pattern. It can be clearly seen that increasing the swivel angle could reduce the total motor cost during the INT phase.

Besides the total motor cost, the estimated natural motor costs, $\mathcal{L}_n$, for different speed and swivel angle changes are shown in Figure 5.3. Same as the total motor

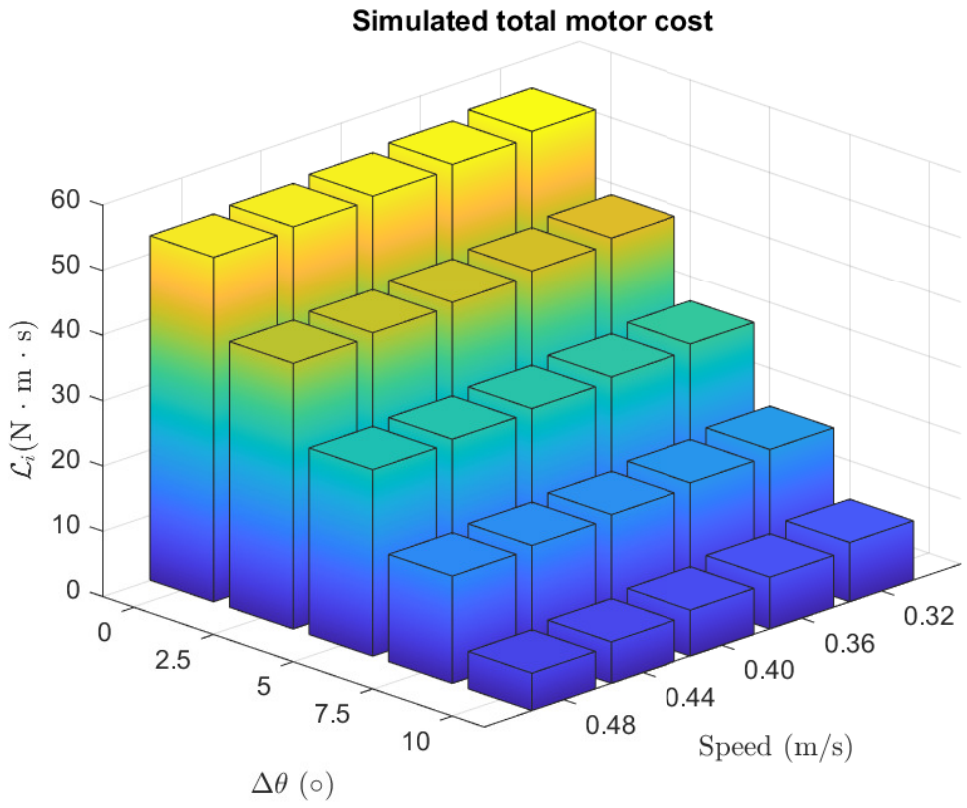

FIGURE 5.2: Simulated motor costs with external force-field calculated as the torque-time integral for different swivel angles and hand movement speeds.

cost, the speed ranges are covered ±10% and ±20% of the average speed, but an exaggerated range of swivel angle change from 0° to 40° is used to make the change of natural cost due to gravity more visible.

5.2.3 Gravity effect

Due to the nature of the task, the natural motor cost is dominated by the gravitational load, which is static by essence: a higher swivel angle will lead to a larger load on shoulder muscles for a given posture. But compared to the cost change induced by the force field when changing the swivel angle, the cost change induced by the gravitational load is weaker (it is noted that the figure shows an exaggerated 40° swivel change to present this cost change). The force-field counteracts the variations of the natural cost regarding the variation of the swivel angle as shown

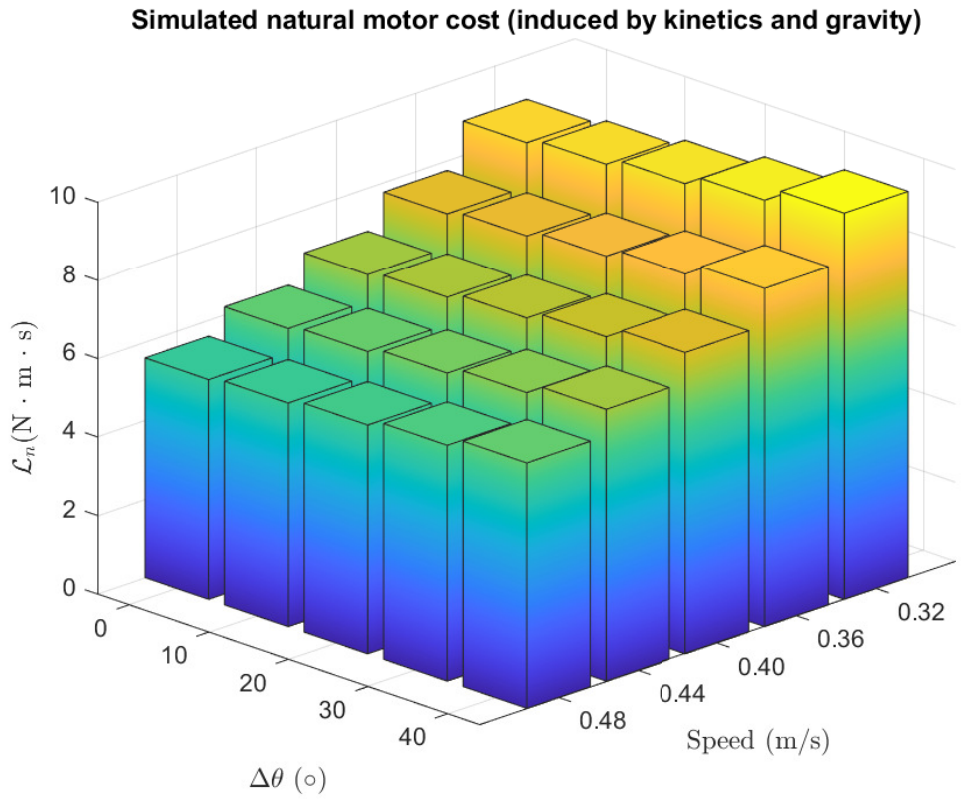

FIGURE 5.3: Simulated motor costs without external force-field calculated as the torque-time integral for different swivel angles and hand movement speeds.

in Figure 5.2. The force-field dominating the overall reaching cost may thus explain why subjects adapt their movement to go towards a new optimal movement cost with a higher swivel angle.

In addition, as illustrated by Figure 5.3, the natural cost, dominated by the gravity, means that a slower movement will require additional energy, as this gravitational load will have to be sustained for a longer time, but this effect of speed is clearly negligible compared to the cost of the force-field (Figure 5.2).

5.3 Motor cost analysis based on experiment data

5.3.1 Data processing

Based on the experiment results, the movement pattern changes during the intervention phase of 20 individuals in two experiments are shown in Figure 5.4. There was one subject in CG group with insignificant change (CG-NS), and the other nine subjects in CG group were with significant change (CG-S). All subjects in PG group were with significant change (PG-S). Thus, all subjects were categorized into three groups as shown in Figure 5.4, where the green, blue, red boxes are corresponding to CG-NS, CG-S, and PG-S groups. To analyze the motor cost changes along with the movement pattern change, experiment data from three

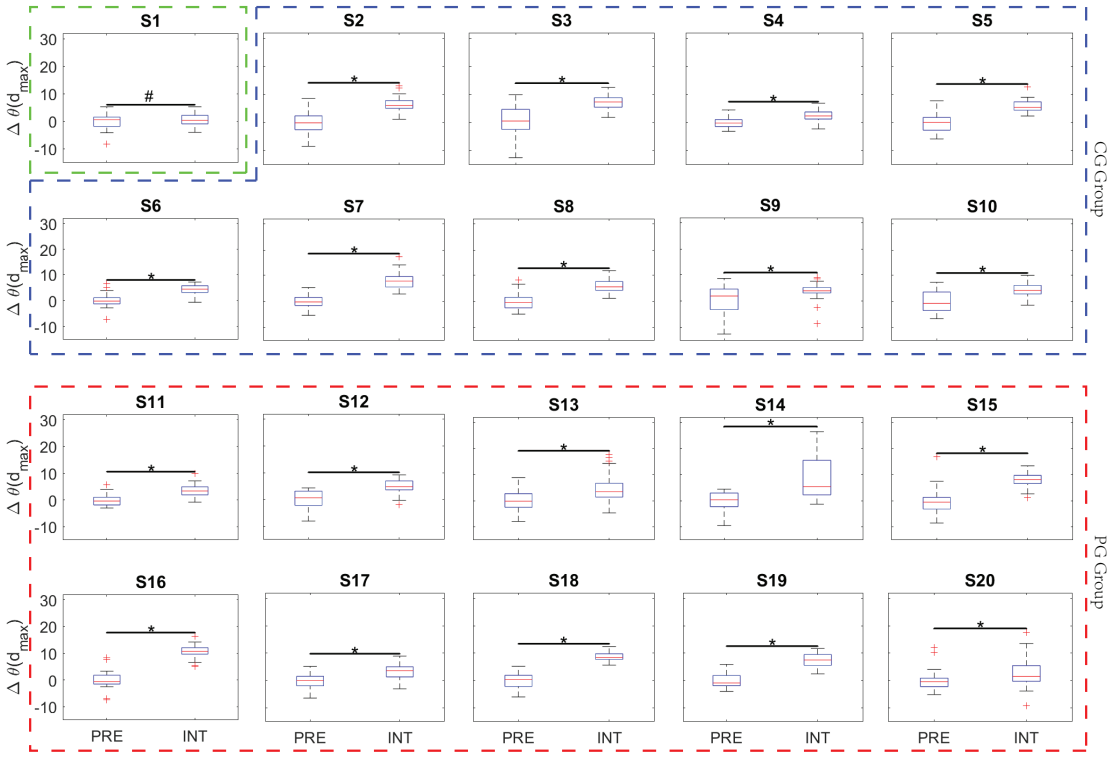

FIGURE 5.4: Individual intervention outcome. The box plot shows individual intervention outcomes in the comparative stage of INT phase (iterations 101 to 135) compared with the PRE phase. Subjects 1 to 10 were in CG group and Subjects 11 to 20 were in PG group. The green, blue, red boxes are corresponding to CG-NS, CG-S, and PG-S groups

subjects who have the closest $\Delta\theta$ compared to the average of the group were chosen from three groups, and the corresponding body parameter measurement and intervention outcome are shown in Table 5.1. In Table 5.1, l_1 and l_2 are measured limb length between joints (shoulder to elbow and elbow to wrist respectively). m_1 and m_2 are estimated limb mass based on the percentage of subjects body weight [89]. And $\Delta\theta(^\circ)$ and ϕ are from measurement from experiment.

TABLE 5.1: Body parameter and intervention outcome of three individuals from three different groups

Group	Subject	l_1 (m)	l_2 (m)	m_1 (kg)	m_2 (kg)	$\Delta\theta(^\circ)$	ϕ
CG-NS	1	0.35	0.33	3.0	2.8	-0.1	-0.09
CG-S	6	0.36	0.29	3.5	3.2	4.4	+0.01
PG-S	14	0.37	0.35	5.1	4.6	5.5	+0.07

5.3.2 Results

The relationship between estimated motor cost and the swivel angle change is presented in Figure 5.5, and the results for three subjects from CG-NS, CG-S, PG-S group are presented in sub-figures (a), (b), and (c) respectively. The motor cost was processed through a sliding-window filter with window size equals ten. The solid blue and red lines illustrate the total motor cost and natural motor cost at corresponding swivel angle changes. With the increase of swivel angle changes, the general trend of the total motor cost is decreased (by 48% in average for three groups), while the natural motor cost has a change by 11% difference in average.

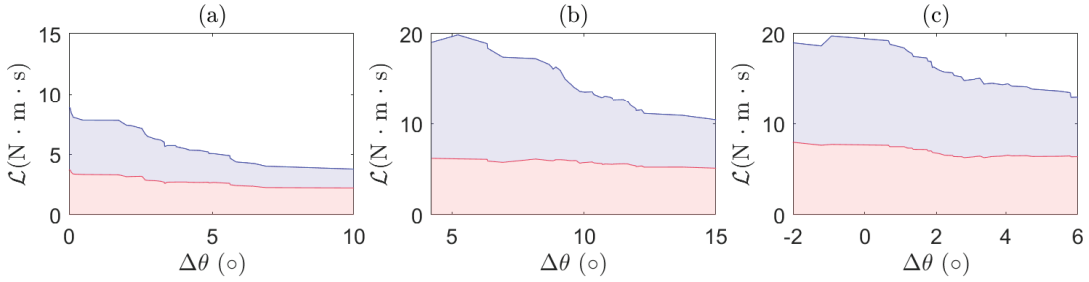

FIGURE 5.5: Estimated motor cost over swivel angle change for (a) CG-NS (b) CG-S (c) PG-S. The solid blue and red lines illustrate the total motor cost and natural motor cost at corresponding swivel angle changes.

Similarly, the relationship between motor cost and hand velocity was shown in Figure 5.6, and the results for three subjects from CG-NS, CG-S, PG-S group are presented in sub-figures (a), (b), and (c) respectively. It can be seen that with the increase of the hand speed, both the total motor cost and natural cost decreased for all three subjects (40% in average for $\mathcal{L}_i$, and 19% in average for $\mathcal{L}_n$).

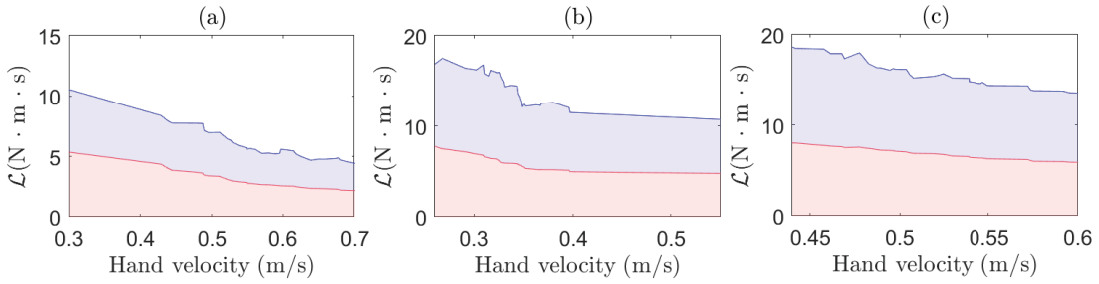

FIGURE 5.6: Estimated motor cost over hand velocity for (a) CG-NS (b) CG-S (c) PG-S.The solid blue and red lines illustrate the total motor cost and natural motor cost at corresponding hand velocity.

5.3.3 Discussion

5.3.3.1 The reason of swivel angle change

In ISC, the goal was to influence the movement pattern through the motor cost change, and thus, the force field was designed in the function of swivel angle. From the experiment result, the total motor cost $\mathcal{L}_i$ is showed to be smaller when the swivel angle increased, and it can be clearly seen that the motor cost induced by the robotic device is dominating the overall cost change. The cost reduction contributed by the robotic device takes more than 77% of total change, and this cost reduction could potentially drive humans to a new optimum, thus explaining the rationale behind the movement pattern change. These results are in agreement with the simulation results as well as the force field design and the hypothesis on the motor cost change.

However, the observation on the change of natural motor cost $\mathcal{L}_n$ is different from both the hypothesis and simulation results. The hypothesis was that the increase of the swivel angle leads to a higher motor cost as the exaggerated pattern requires

a higher load at the shoulder to produce more work to compensate for the gravity. The simulation results validated this hypothesis. However, in the experiment results, the natural cost decreased when the swivel angle increased, although the change is small (around 10%). It is noted that the simulation results isolate the influence from the hand velocity changes when presenting the relationship between the natural motor cost and swivel angle, but the experiment results do not. So this small perturbation could potentially come from the influence of hand velocity rather than the swivel angle. Although the trend is different between simulation and experiment results, both agree that the swivel angle influences the natural motor cost weakly.

It can still be seen that the average swivel angle "reached" by both groups introduced in the real experiment is below the shaping goal at which the force-field component in the cost function would become zero, suggesting that subjects do not fully reach an optimal behaviour, or that some elements of the cost are not captured in this simulation.

5.3.3.2 Effect of hand velocity

Besides the swivel angle change, the motor cost was also influenced by the hand velocity. The experiment results show that the increase of hand velocity leads to reductions in both natural motor cost and total motor cost. These results are in agreement with the simulation results. The analysis shows that total motor cost has a 40% reduction in average, and the natural motor cost contributes half of this change (19%), while the rest half is contributed by the cost induced by the robotic device.

There exists a cost compromise between the motor cost and hand velocity. Due to the nature of the viscous force field, the higher velocity induces a higher force field and leads to a higher motor cost, but in contrast, it reduces the duration to complete the task and results in a lower accumulated motor cost in completing the task.

An interesting observation in the experiment is that subjects in both groups reduced their velocity magnitude, of 16% and 20% respectively for the CG and PG groups in the majority of iterations (see Figure 4.5). A possible explanation for this is that the subjects tried to limit the instantaneous force field effect by reducing their speed, independently of the overall movement cost. Indeed although the cost due to the force-field is itself unaffected by the movement time, the instantaneous intensity of the force is. The anatomic structure could be another factor in this cost analysis. For example, a lighter arm with weaker muscle could be sensitive to the instantaneous force field but cost less due to the gravity. It may result in a slower movement to accept an accumulated cost against a high instantaneous cost. Due to there being no muscle analysis in this experiment, this is an interesting point to be investigated in the future study.

5.4 Summary

This cost analysis explained the observation in the experiment and proved the effectiveness of the force field (ISC) introduced in the experiment. Both the experiment results and simulated results illustrate the fact that in this experiment, the cost involved by the force field was clearly acting in the opposite direction of the gravitational load and clearly dominating it. This model helps to interpret the experimental results. However, this model still needs further improvement as it does not take into account the actual muscle distribution and assumed each joint has an equal contribution in the total cost, which cannot be confirmed in most scenarios. A detailed model could potentially provide a more accurate estimation of motor cost change, and as such, the force field could be further improved quantitatively based on the motor cost estimation.

Chapter 6

Conclusion

This thesis aims to investigate the feasibility of shaping human's movement pattern using a simpler device. Three topics were investigated in this thesis: a) the feasibility of shaping healthy subjects' movement patterns using a physical intervention produced by robotics device in an indirect and implicit manner; b) the contribution of a progressively changing goal in this implicit motor adaptation, assuming that this adaptation may be further promoted through subtle prompts to explore the cost space; c) a cost analysis based on the upper limb kinematics and dynamics model to validate the relationship between observations and motor cost.

6.1 Contributions

First, the major contribution of this thesis is confirming the feasibility of inducing human motor adaptation solely relying on motor cost with the absence of kinematics error. The experiment results suggested that influencing human motor cost through applying a force field in null space could favor an adaptation in redundant space towards the desired pattern. This finding empowers simple robotic devices such as manipulandum devices to be used in movement pattern shaping for highly redundant tasks.

Secondly, leveraging the principle of neuroplasticity, a hypothesis that a progressive goal could improve the shaping outcome was proposed and tested by deploying the progressivity into the force field used in the previous experiment. The results confirmed the feasibility of inducing human movement pattern change with an indirect force field. But, surprisingly, the results suggested that the progressivity used in this experiment didn't drive a significant improvement in the outcome.

Finally, a motor cost analysis was performed to explore the relationship between the observations (swivel angle and hand velocity) and motor cost. The results showed that a higher swivel angle could lead to a lower total motor cost which proved the rationality of the design of the force field and explained the side effect on hand velocity change observed in the experiment.

6.2 Limitations and future work

Movement pattern shaping shows high demand in different fields. Especially in neurorehabilitation, the impairment in motor function brings significant limitations on stroke survivors' quality of life. Under the general trend of aging in most developed countries, the demand for neurorehabilitation is expected to be even higher in the next few decades, thus making the studies on movement pattern shaping critical. As shown in the results, this shaping strategy could shape human movement patterns by influencing the human motor cost. Regrettably, no after effect and retention were observed in this study, suggesting that the subjects quickly came back to their original movement pattern when the force field was removed. The chosen task and problem in this study aim to be relevant to motor neuro-rehabilitation of the upper limb, where pathological synergies retraining and movement correction play an important role towards functional recovery. But in this study, after effect was not expected to happen, as the desired exaggerated new movement pattern leads to a higher cost and subjects do not gain any benefit from this new movement pattern when they are moving without the artificial force field. If the newly learned movement pattern is beneficial to the subjects, the after effect

and retention are expected to happen as in neurorehabilitation training. Also, in the most of similar motor learning studies, the force field is suddenly removed to better observe the after effect which usually lasts for a few iterations. In this experiment, to keep the subject unaware of the force field, the intervention was removed progressively which led to a lost opportunity to observe a clean after effect. The current study is still under laboratory conditions and tested with healthy subjects. To further explore the effectiveness of this strategy in neurorehabilitation training, a clinical evaluation of the feasibility for individuals with neurological injury is required.

The extensibility of this shaping strategy is an exciting research topic in the future study. Due to the high redundancy of the human's muscle-skeletal system, human can have different muscle activation patterns at the same kinematic state. In this case, observation at the muscle level can provide more information directly and accurately compared to observation at the joint level. Besides, in neurorehabilitation, the reactivation of the primary brain lesion area is not expected, and the neurorehabilitation therapy of post-stroke mainly aims to generate activation in alternative brain areas not normally observed in non-disabled individuals [79]. While the muscles are activated by the neural system directly, it is believed that shaping specific muscle activation can be beneficial to encourage neural rewiring and function relearning in the neuro-rehab process. In addition, due to many everyday tasks are intrinsically unstable and so different muscle activation for the same posture/movement (*i.e.* keeping a screwdriver in the slot of a screw is unstable [22]), stability may be dependent on the control of mechanical impedance in the human arm. To empower patients' abilities to perform these common tasks in their daily lives, the joint level shaping is insufficient. So the feasibility of inducing the muscle activation pattern change using physical intervention produced by robotic devices become an exciting research topic in the future study.

In addition, the movement pattern was characterised by the swivel angle in this study, but the results suggested that movement time and speed are also important parameters in the movement pattern and motor cost. The simulation results

demonstrated the potential of shaping the movement speed in an indirect and implicit manner. Considering performing the same movement but at different speeds could lead to different results in many sports (i.e. swinging a golf club or throwing a ball), it has broad applications in sports training. In this case, a different cost, the performance, could be introduced. It will be an interesting topic to investigate the compromise between energy expenditure and performance, which has a good potential to provide a minimum-motor-cost training process for athletes.

Besides this, the progressivity in the second experiment was set to a constant linear goal without considering the differences among subjects. Thus, the personalization of this force field is also worth investigating. From the observation of the experiment, the shaping outcome varies from person to person largely. Given that different persons have different muscle content and learning steps, the outcome could be improved if the force field could adapt to different subjects based on the iterative performance data (or additional information). The tuning gain of the magnitude of the force field was set as a constant number in this experiment, and it resulted in the same force feedback for different subjects if they performed the same kinematics trajectory. This parameter has the potential to be an iterative learnable parameter contributing to personalization.

The last point to be further improved in future is a detailed human motor cost analysis with more observations and a detailed model. The current model cannot precisely describe the real motor cost change during the experiment, as it did not take the muscle distribution into account. And the assumptions on equivalent cost contribution from torque at each joint could not be realistic in most cases. In this case, a better model and a detailed simulation could contribute to a better understanding of the relationship between swivel angle change and motor cost change, thus contributing to the design of an intervention to achieve a better outcome.

Bibliography

[1] J. Fong. *Computational models of human motor movement and learning and their application to neurorehabilitation*. PhD thesis, Department of Mechanical Engineering, School of Engineering, THE UNIVERSITY OF MELBOURNE, 2017.

[2] P. Garrec, J. Friconneau, Y. Measson, and Y. Perrot. Able, an innovative transparent exoskeleton for the upper-limb. In *2008 IEEE/RSJ International Conference on Intelligent Robots and Systems*, pages 1483–1488. IEEE, 2008.

[3] T. Nef, M. Mihelj, and R. Riener. Armin: a robot for patient-cooperative arm therapy. *Medical & Biological Engineering & Computing*, 45:887–900, August 2007. doi: 10.1007/s11517-007-0226-6. URL https://doi.org/10.1007/s11517-007-0226-6.

[4] E. B. Brokaw, T. Murray, T. Nef, and P. S. Lum. Retraining of interjoint arm coordination after stroke using robot-assisted time-independent functional training. *Journal of Rehabilitation Research and Development*, 48(4):299–316, 2011. doi: 10.1682/JRRD.2010.04.0064. URL https://doi.org/10.1682/JRRD.2010.04.0064.

[5] T. Proietti, E. Guigon, A. Roby-Brami, and N. Jarrassé. Modifying upper-limb inter-joint coordination in healthy subjects by training with a robotic exoskeleton. *Journal of NeuroEngineering and Rehabilitation*, 14(1):1–19, June 2017. doi: 10.1186/s12984-017-0254-x. URL https://doi.org/10.1186/s12984-017-0254-x.

[6] J. Hidler, D. Nichols, M. Pelliccio, and K. Brady. Advances in the understanding and treatment of stroke impairment using robotic devices. *Topics in stroke rehabilitation*, 12(2):22–35, February 2005. URL https://doi.org/10.1310/RYT5-62N4-CTVX-8JTE.

[7] C. G. Burgar, P. S. Lum, P. C. Shor, and H. F. Machiel Van der Loos. Development of robots for rehabilitation therapy: The palo alto va/stanford experience. *Journal of rehabilitation research and development*, 37(6):663–674, December 2000.

[8] E. B. Brokaw, P. S. Lum, R. A. Cooper, and B. R. Brewer. Using the kinect to limit abnormal kinematics and compensation strategies during therapy with end effector robots. In *2013 IEEE 13th International Conference on Rehabilitation Robotics (ICORR)*, pages 1–6, Seattle, WA, USA, June 2013. doi: 10.1109/ICORR.2013.6650384. URL https://doi.org/10.1109/ICORR.2013.6650384.

[9] J. Perl. A neural network approach to movement pattern analysis. *Human Movement Science*, 23(5):605–620, November 2004. doi: 10.1016/j.humov.2004.10.010. URL https://doi.org/10.1016/j.humov.2004.10.010.

[10] G. Wulf and C. H. Shea. Principles derived from the study of simple skills do not generalize to complex skill learning. *Psychonomic bulletin & review*, 9(2):185–211, June 2002. doi: doi.org/10.3758/BF03196276. URL https://doi.org/10.3758/BF03196276.

[11] World Health Organization. Stroke, cerebrovascular accident. http://www.emro.who.int/health-topics/stroke-cerebrovascular-accident/index.html, 2021. Accessed: 2021-06-30.

[12] E. S. Donkor. Stroke in the century: a snapshot of the burden, epidemiology, and quality of life. *Stroke research and treatment*, 2018, 2018. doi: 10.1155/2018/3238165. URL https://doi.org/10.1155/2018/3238165.

[13] Australian Bureau of Statistics. 2018 survey of disability, ageing and carers. https://www.abs.gov.au/statistics/health/disability/disability-ageing-and-carers-australia-summary-findings/2018, 2019. Accessed: 2021-06-30.

[14] Australian Institution of Health and Welfare. Australia's health 2020: Stroke. https://www.aihw.gov.au/reports/australias-health/stroke, 2020. Accessed: 2021-06-30.

[15] M. F. Levin, J. A. Kleim, and S. L. Wolf. What do motor "recovery" and "compensationg" mean in patients following stroke? *Neurorehabilitation and Neural Repair*, 23(4):313–319, May 2009. doi: 10.1177/1545968308328727. URL https://doi.org/10.1177/1545968308328727.

[16] G. B. Salsich, V. Graci, and D. E. Maxam. The effects of movement pattern modification on lower extremity kinematics and pain in women with patellofemoral pain. *Journal of Orthopaedic & Sports Physical Therapy*, 42(12):1017–1024, December 2012. doi: 10.2519/jospt.2012.4231. URL https://doi.org/10.2519/jospt.2012.4231.

[17] C. L. Lewis, A. Khuu, and L. N. Marinko. Postural correction reduces hip pain in adult with acetabular dysplasia: a case report. *Manual Therapy*, 20(3):508–512, June 2015. doi: 10.1016/j.math.2015.01.014. URL https://doi.org/10.1016/j.math.2015.01.014.

[18] J. E. Earl and C. S. Vetter. Patellofemoral pain. *Physical Medicine and Rehabilitation Clinics of North America*, 18(3):439–458, August 2007. doi: 10.1016/j.pmr.2007.05.004. URL https://doi.org/10.1016/j.pmr.2007.05.004.

[19] M. G. Allison and T. Ayllon. Behavioral coaching in the development of skills in football, gymnastics, and tennis. *Journal of Applied Behavior Analysis*, 13 (2):297–314, 1980. doi: 10.1901/jaba.1980.13-297. URL https://doi.org/10.1901/jaba.1980.13-297.

[20] T. D. Lee and L. R. Wishart. Motor learning conundrums (and possible solutions). *Quest*, 57(1):67–78, April 2005. doi: 10.1080/00336297.2005.10491843. URL https://doi.org/10.1080/00336297.2005.10491843.

[21] C. J. Winstein and D. B. Kay. Chapter 16 - translating the science into practice: shaping rehabilitation practice to enhance recovery after brain damage. In N. Dancause, S. Nadeau, and S. Rossignol, editors, *Sensorimotor Rehabilitation*, volume 218 of *Progress in Brain Research*, pages 331–360. Elsevier, 2015. URL https://doi.org/10.1016/bs.pbr.2015.01.004.

[22] E. Burdet, R. Osu, D. W. Franklin, T. E. Milner, and M. Kawato. The central nervous system stabilizes unstable dynamics by learning optimal impedance. *Nature*, 414:446–449, November 2001.

[23] A. McMorland, K. D. Runnalls, and W. D. Byblow. A neuroanatomical framework for upper limb synergies after stroke. *Frontiers in Human Neuroscience*, 9:82, 2015. ISSN 1662-5161. doi: 10.3389/fnhum.2015.00082. URL https://www.frontiersin.org/article/10.3389/fnhum.2015.00082.

[24] T. Flash and N. Hogan. The coordination of arm movements: an experimentally confirmed mathematical model. *Journal of Neuroscience*, 5(7): 1688–1703, 1985. doi: 10.1523/jneurosci.05-07-01688.1985. URL https://doi.org/10.1523/jneurosci.05-07-01688.1985.

[25] H. Kim, L. M. Miller, N. Byl, G. M. Abrams, and J. Rosen. Redundancy resolution of the human arm and an upper limb exoskeleton. *IEEE Transactions on Biomedical Engineering*, 59(6):1770–1779, April 2012. doi: 10.1109/TBME.2012.2194489. URL https://doi.org/10.1109/TBME.2012.2194489.

[26] T. Kang, J. He, and S. I. H. Tillery. Determining natural arm configuration along a reaching trajectory. *Experimental brain research*, 167(3):352–361, October 2005. doi: 10.1007/s00221-005-0039-5. URL https://doi.org/10.1007/s00221-005-0039-5.

[27] Y. Uno, M. Kawato, and R. Suzuki. Formation and control of optimal trajectory in human multijoint arm movement. *Biological Cybernetics*, 61(2): 89–101, June 1989. doi: 10.1007/BF00204593. URL https://doi.org/10.1007/BF00204593.

[28] E. Nakano, H. Imamizu, R. Osu, Y. Uno, H. Gomi, T. Yoshioka, and M. Kawato. Quantitative examinations of internal representations for arm trajectory planning: minimum commanded torque change model. *Journal of Neurophysiology*, 81(5):2140–2155, 1999.

[29] E. Guigon, P. Baraduc, and M. Desmurget. Computational motor control: Redundancy and invariance. *Journal of Neurophysiology*, 97(1):331–347, January 2007. doi: 10.1152/jn.00290.2006. URL https://doi.org/10.1152/jn.00290.2006.

[30] E. Todorovand and M. I. Jordan. Optimal feedback control as a theory of motor coordination. *Nature neuroscience*, 5(11):1226–1235, 2002.

[31] D. Liu and E. Todorov. Evidence for the flexible sensorimotor strategies predicted by optimal feedback control. *Journal of Neuroscience*, 27(35):9354–9368, 2007. ISSN 0270-6474. doi: 10.1523/JNEUROSCI.1110-06.2007. URL https://www.jneurosci.org/content/27/35/9354.

[32] C. M. Harris and D. M. Wolpert. Signal-dependent noise determines motor planning. *Nature*, 394:780–784, August 1998. doi: 10.1038/29528. URL https://doi.org/10.1038/29528.

[33] D. Tolani and N. I. Badler. Real-time inverse kinematics of the human arm. *Presence: Teleoperators and Virtual Environments*, 5(4):393–401, 11 1996. doi: 10.1162/pres.1996.5.4.393. URL https://doi.org/10.1162/pres.1996.5.4.393.

[34] N. Qian, Y. Jiang, Z. Jiang, and P. Mazzoni. Movement duration, fitts's law, and an infinite-horizon optimal feedback control model for biological motor

systems. *Neural Computation*, 25(3):697–724, March 2013. doi: 10.1162/NECO_a_00410. URL https://doi.org/10.1162/NECO_a_00410.

[35] J. W. Krakauer. Motor learning: its relevance to stroke recovery and neurorehabilitation. *Current opinion in neurology*, 19(1):84–90, February 2006. doi: 10.1097/01.wco.0000200544.29915.cc. URL https://doi.org/10.1097/01.wco.0000200544.29915.cc.

[36] T. Kitago and J. W. Krakauer. Motor learning principles for neurorehabilitation. *Handbook of clinical neurology*, 110:93–103, 2013. doi: 10.1016/B978-0-444-52901-5.00008-3. URL https://doi.org/10.1016/B978-0-444-52901-5.00008-3.

[37] V. S. Huang and J. W. Krakauer. Robotic neurorehabilitation: a computational motor learning perspective. *Journal of neuroengineering and rehabilitation*, 6(1):1–13, February 2009.

[38] O. Hikosaka K. Nakamura, K. Sakai, and H. Nakahara. Central mechanisms of motor skill learning. *Current opinion in neurobiology*, 12(2): 217–222, April 2002. doi: 10.1016/S0959-4388(02)00307-0. URL https://doi.org/10.1016/S0959-4388(02)00307-0.

[39] J. E. Mazur and R. Hastie. Learning as accumulation: A reexamination of the learning curve. *Psychological bulletin*, 85(6):1256, 1978.

[40] A. T. Welford. On rates of improvement with practice. *Journal of Motor Behavior*, 19(3):401–415, February 1987.

[41] K. M. Newell, Y. Liu, and G. Mayer-Kress. Time scales in motor learning and development. *Psychological review*, 108(1):57, 2001.

[42] G. S. Snoddy. Learning and stability: a psychophysiological analysis of a case of motor learning with clinical applications. *Journal of Applied Psychology*, 10(1):1, 1926.

[43] K. Doya. Complementary roles of basal ganglia and cerebellum in learning and motor control. *Current opinion in neurobiology*, 10(6):732–739, December 2000.

[44] J. L. Emken, R. Benitez, A. Sideris, J. E. Bobrow, and R. J. David. Motor adaptation as a greedy optimization of error and effort. *Journal of Neurophysiology*, 97(6):3997–4006, June 2007. doi: 10.1152/jn.01095.2006. URL https://doi.org/10.1152/jn.01095.2006.

[45] S. Zhou, D. Oetomo, Y. Tan, E. Burdet, and I. Mareels. Modeling individual human motor behavior through model reference iterative learning control. *IEEE Transactions on Biomedical Engineering*, 59(7):1892–1901, July 2012.

[46] S. Zhou, Y. Tan, D. Oetomo, C. Freeman, E. Burdet, and I. Mareels. Modeling of endpoint feedback learning implemented through point-to-point learning control. *IEEE Transactions on Control Systems Technology*, 25(5):1576–1585, September 2016.

[47] S. Cheng and P. N. Sabes. Modeling sensorimotor learning with linear dynamical systems. *Neural computation*, 18(4):760–793, April 2006.

[48] K. A. Thoroughman, M. S. Fine, and J. A. Taylor. Trial-by-trial motor adaptation: a window into elemental neural computation. *Progress in brain research*, 165:373–382, 2007. URL https://doi.org/10.1016/S0079-6123(06)65023-1.

[49] Y. Ueyama. System identification of neural mechanisms from trial-by-trial motor behaviour: modelling of learning, impairment and recovery. *Advanced Robotics*, 31(3):107–117, December 2017. URL https://doi.org/10.1080/01691864.2016.1266966.

[50] N. Bhushan and R. Shadmehr. Computational nature of human adaptive control during learning of reaching movements in force fields. *Biological cybernetics*, 81(1):39–60, July 1999. URL https://doi.org/10.1007/s004220050543.

[51] Y. Jiang and Z. Jiang. Adaptive dynamic programming as a theory of sensorimotor control. *Biological Cybernetics*, 108(4):459–473, June 2014. doi: 10.1007/s00422-014-0613-7. URL https://doi.org/10.1007/s00422-014-0613-7.

[52] J. Izawa, T. Rane, O. Donchin, and R. Shadmehr. Motor adaptation as a process of reoptimization. *Journal of Neuroscience*, 28(11):2883–2891, March 2008. doi: 10.1523/JNEUROSCI.5359-07.2008. URL https://doi.org/10.1523/JNEUROSCI.5359-07.2008.

[53] Y. R. Miyamoto, S. Wang, and M. A. Smith. Implicit adaptation compensates for erratic explicit strategy in human motor learning. *Nature neuroscience*, 23(3):443–455, 2020.

[54] L. R. Squire. Chapter 7 - memory and brain. In S. L. Friedman, K. A. Klivington, and R. W. Peterson, editors, *The brain, cognition, and education*. Academic Press, INC, 1987.

[55] C. A. Seger. Implicit learning. *Psychological bulletin*, 115(2):163, 1994.

[56] T. D. Green and J. H. Flowers. Implicit versus explicit learning processes in a probabilistic, continuous fine-motor catching task. *Journal of motor behavior*, 23(4):293–300, 1991.

[57] B. L. Benson, J. A.Anguera, and R. D. Seidler. A spatial explicit strategy reduces error but interferes with sensorimotor adaptation. *Journal of neurophysiology*, 105(6):2843–2851, 2011.

[58] L. S. Jakobson and M. A. Goodale. Trajectories of reaches to prismatically-displaced targets: evidence for "automatic" visuomotor recalibration. *Experimental brain research*, 78(3):575–587, 1989.

[59] J. L. Patton and F. A. Mussa-Ivaldi. Robot-assisted adaptive training: Custom force fields for teaching movement patterns. *IEEE Transactions on Biomedical Engineering*, 51(4):636–646, March 2004. doi: 10.1109/TBME.2003.821035. URL https://doi.org/10.1109/TBME.2003.821035.

[60] M. A. Smith and R. Shadmehr. Intact ability to learn internal models of arm dynamics in huntington's disease but not cerebellar degeneration. *Journal of neurophysiology*, 93(5):2809–2821, 2005.

[61] M. A. Smith, A. Ghazizadeh, and R. Shadmehr. Interacting adaptive processes with different timescales underlie short-term motor learning. *PLOS Biology*, 4(6):1035–1043, May 2006. doi: 10.1371/journal.pbio.0040179. URL https://doi.org/10.1371/journal.pbio.0040179.

[62] W. M. Joiner and M. A. Smith. Long-term retention explained by a model of short-term learning in the adaptive control of reaching. *Journal of neurophysiology*, 100(5):2948–2955, 2008.

[63] M. J. Wagner and M. A. Smith. Shared internal models for feedforward and feedback control. *Journal of Neuroscience*, 28(42):10663–10673, 2008.

[64] G. C. Sing, W. M. Joiner, T. Nanayakkara, J. B. Brayanov, and M. A. Smith. Primitives for motor adaptation reflect correlated neural tuning to position and velocity. *Neuron*, 64(4):575–589, 2009.

[65] L. A. Boyd and C. J. Winstein. Implicit motor-sequence learning in humans following unilateral stroke: the impact of practice and explicit knowledge. *Neuroscience letters*, 298(1):65–69, 2001.

[66] P. Mazzoni and J. W. Krakauer. An implicit plan overrides an explicit strategy during visuomotor adaptation. *Journal of neuroscience*, 26(14):3642–3645, 2006.

[67] J. Fong, V. Crocher, Y. Tan, D. Oetomo, and I. Mareels. Emu: A transparent 3d robotic manipulandum for upper-limb rehabilitation. In *2017 International Conference on Rehabilitation Robotics (ICORR)*, pages 771–776, London, UK, July 2017. IEEE. doi: 10.1109/ICORR.2017.8009341. URL https://doi.org/10.1109/ICORR.2017.8009341.

[68] N. Hogan, H. I. Krebs, J. Charnnarong, P. Srikrishna, and A. Sharon. Mitmanus: a workstation for manual therapy and training. i. In *[1992] Proceedings IEEE International Workshop on Robot and Human Communication*, pages 161–165. IEEE, August 1992. URL https://doi.org/10.1109/ROMAN.1992.253895.

[69] D. J. Reinkensmeyer and J. L. Patton. Can robots help the learning of skilled actions? *Exercise and sport sciences reviews*, 37(1):43, January 2009. URL https://doi.org/10.1097/JES.0b013e3181912108.

[70] G. Kwakkel, B. J. Kollen, and H. I. Krebs. Effects of robot-assisted therapy on upper limb recovery after stroke: a systematic review. *Neurorehabilitation and neural repair*, 22(2):111–121, September 2008. URL https://doi.org/10.1177/1545968307305457.

[71] G. B. Prange, M. J .A. Jannink, C. G. M. Groothuis-Oudshoorn, H. J. Hermens, and M. J. Ijzerman. Systematic review of the effect of robot-aided therapy on recovery of the hemiparetic arm after stroke. *Journal of Rehabilitation Research and Development*, 43(2):171–184, 2009.

[72] D. Feygin, M. Keehner, and R. Tendick. Haptic guidance: Experimental evaluation of a haptic training method for a perceptual motor skill. In *Proceedings 10th Symposium on Haptic Interfaces for Virtual Environment and Teleoperator Systems. HAPTICS 2002*, pages 40–47. IEEE, March 2002. URL https://doi.org/10.1109/HAPTIC.2002.998939.

[73] J. Liu, S. C. Cramer, and D. J. Reinkensmeyer. Learning to perform a new movement with robotic assistance: comparison of haptic guidance and visual demonstration. *Journal of neuroengineering and rehabilitation*, 3(1):1–10, August 2006. URL https://doi.org/10.1186/1743-0003-3-20.

[74] B. A. Valdés, A. N. Schneider, and H. F. M. Van der Loos. Reducing trunk compensation in stroke survivors: A randomized crossover trial comparing visual and force feedback modalities. *Archives of Physical Medicine and Rehabilitation*, 98(10):1932–1940, October 2017. doi: 10.1016/j.apmr.2017.03.034. URL https://doi.org/10.1016/j.apmr.2017.03.034.

[75] S. Micera, J. Carpaneto, F. Posteraro, L. Cenciotti, M. Popovicc, and P. Dario. Characterization of upper arm synergies during reaching tasks in able-bodied and hemiparetic subjects. *Clinical Biomechanics*, 20(9): 939–946, November 2005. doi: 10.1016/j.clinbiomech.2005.06.004. URL https://doi.org/10.1016/j.clinbiomech.2005.06.004.

[76] J. Fong, V. Crocher, Y. Tan, and D. Oetomo. Indirect robotic movement shaping through motor cost influence. In *2019 IEEE 16th International Conference on Rehabilitation Robotics (ICORR)*, pages 977–982, Toronto, ON, Canada, June 2019. doi: 10.1109/icorr.2019.8779430. URL https://doi.org/10.1109/icorr.2019.8779430.

[77] V. Crocher, J. Fong, T. J. Bosch, Y. Tan, I. Mareels, and D. Oetomo. Upper limb deweighting using underactuated end-effector-based backdrivable manipulanda. *IEEE Robotics and Automation Letters*, 3(3):2116–2122, July 2018. doi: 10.1109/LRA.2018.2809605. URL https://doi.org/10.1109/LRA.2018.2809605.

[78] W. J. Conover. *Practical nonparametric statistics*, volume 350. john wiley & sons, 1999.

[79] M. F. Levin. Interjoint coordination during pointing movements is disrupted in spastic hemiparesis. *Brain*, 119(1):281–293, February 1996. doi: 10.1093/brain/119.1.281. URL https://doi.org/10.1093/brain/119.1.281.

[80] B. A. Valdés and H. F. M. Van der Loos. Biofeedback vs. game scores for reducing trunk compensation after stroke: a randomized crossover trial. *Topics in Stroke Rehabilitation*, 25(2):96–113, October 2017. doi: 10.1080/10749357.2017.1394633. URL https://doi.org/10.1080/10749357.2017.1394633.

[81] M. Nahum, H. Lee, and M. M. Merzenich. Chapter 6 - principles of neuroplasticity-based rehabilitation. In M. M. Merzenich, M. Nahum, and T. M. Van Vleet, editors, *Changing Brains*, volume 207 of *Progress in Brain Research*, pages 141–171. Elsevier, 2013. doi: 10.1016/B978-0-444-63327-9.00009-6. URL https://doi.org/10.1016/B978-0-444-63327-9.00009-6.

[82] V. Crocher, A. Sahbani, J. Robertson, A. Roby-Brami, and G. Morel. Constraining upper limb synergies of hemiparetic patients using a robotic exoskeleton in the perspective of neuro-rehabilitation. *IEEE Transactions on Neural Systems and Rehabilitation Engineering*, 20(3):247–257, April 2012. ISSN 15344320. doi: 10.1109/TNSRE.2012.2190522. URL https://doi.org/10.1109/TNSRE.2012.2190522.

[83] G. Aston-Jones and J. D. Cohen. An integrative theory of locus coeruleus-norepinephrine function: adaptive gain and optimal performance. *Annual Review of Neuroscience*, 28:403–450, July 2005. URL https://doi.org/10.1146/annurev.neuro.28.061604.135709.

[84] S. J. Sara. The locus coeruleus and noradrenergic modulation of cognition. *Nature reviews neuroscience*, 10(3):211–223, February 2009. URL https://doi.org/10.1016/j.neuron.2012.09.011.

[85] S. J. Sara and S. Bouret. Orienting and reorienting: the locus coeruleus mediates cognition through arousal. *Neuron*, 76(1):130–141, 2012.

[86] M. Casadio and V. Sanguineti. Learning, retention, and slacking: A model of the dynamics of recovery in robot therapy. *IEEE Transactions on Neural Systems and Rehabilitation Engineering*, 20(3):286–296, April 2012. doi: 10.1109/TNSRE.2012.2190827. URL https://doi.org/10.1109/TNSRE.2012.2190827.

[87] V. Rozand, T. Cattagni, J. Theurel, A. Martin, and R. Lepers. Neuromuscular fatigue following isometric contractions with similar torque time integral. *International journal of sports medicine*, 36(01):35–40, 2015.

[88] RL Williams. Engineering biomechanics of human motion. *NotesBook Supplement for ME 4670/BME*, 5670, 2014.

[89] S. Plagenhoef, F. G. Evans, and T. Abdelnour. Anatomical data for analyzing human motion. *Research quarterly for exercise and sport*, 54(2):169–178, June 1983. URL https://doi.org/10.1080/02701367.1983.10605290.